

# Wilson network decomposition of AdS Feynman diagrams in two dimensions

---

**Konstantin Alkalaev<sup>a,b</sup> and Vladimir Khiteev<sup>a</sup>**

<sup>a</sup>*I.E. Tamm Department of Theoretical Physics,  
P.N. Lebedev Physical Institute, 119991 Moscow, Russia*

<sup>b</sup>*Institute for Theoretical and Mathematical Physics,  
Lomonosov Moscow State University, 119991 Moscow, Russia*

*E-mail:* [alkalaev@lpi.ru](mailto:alkalaev@lpi.ru), [khiteev@lpi.ru](mailto:khiteev@lpi.ru)

**ABSTRACT:** We show that Feynman diagrams in  $\text{AdS}_2$  space can be decomposed into infinite series of matrix elements of Wilson line network operators. The case of the 3-point scalar Feynman diagram with endpoints in the bulk is studied in detail. The resulting decomposition is similar to the conformal block decomposition of Witten diagrams, i.e. it comprises a single-trace term and infinite sums of double-trace terms. We derive a number of AdS propagator identities which relate the standard bulk-to-bulk propagators with the modified bulk-to-bulk propagators of two different types responsible for extracting single-trace and double-trace terms.

---

## Contents

<b>1</b>	<b>Introduction</b>	<b>1</b>
<b>2</b>	<b>HKLL reconstruction and Witten diagrams</b>	<b>4</b>
2.1	Reconstruction formula	4
2.2	Conformal block decomposition	5
<b>3</b>	<b>AdS integral identities and modified propagators</b>	<b>7</b>
3.1	Three identities	8
3.2	Modified AdS Feynman diagrams	9
3.3	Commentary	12
<b>4</b>	<b>Wilson network decomposition of AdS Feynman diagrams</b>	<b>13</b>
4.1	Wilson networks as basis functions	13
4.2	Deriving the Wilson network decomposition	14
4.2.1	Single-trace contributions	15
4.2.2	Double-trace contributions	16
4.2.3	Superposition identity	20
<b>5</b>	<b>Conclusion and outlooks</b>	<b>23</b>
<b>A</b>	<b>Analytic continuation of the 3-point Witten diagram</b>	<b>23</b>
<b>B</b>	<b>Proofs of lemmas</b>	<b>26</b>
B.1	Lemma 1	26
B.2	Lemma 2	27
B.3	Lemma 3	31
B.4	Lemma 4	36
B.5	Lemma 5	37

---

## 1 Introduction

Feynman diagrams in AdS space are built in the same way as in Minkowski space. All the basic principles of representing particles and their interactions with lines and vertices remain intact, with the only significant exception being that each particle can propagate in three distinct regimes: bulk-to-bulk, bulk-to-boundary, boundary-to-boundary. Of course, this multiplication of propagation types is directly related to the existence of the conformal boundary of AdS space endowed with the causal structure. This phenomenon underlies the

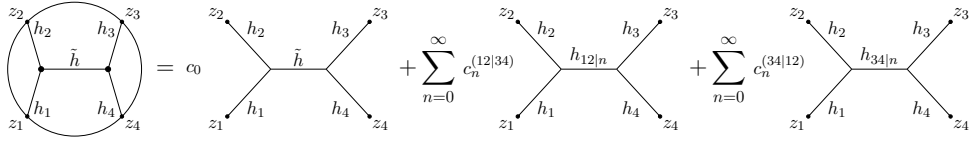


**Figure 1.** The conformal block decomposition of the 4-point exchange Witten diagram. On the left-hand side: there are four scalars of masses  $m_i^2 = h_i(h_i - 1)$ ,  $i = 1, \dots, 4$ , and one exchange scalar of mass  $\tilde{m}^2 = \tilde{h}(\tilde{h} - 1)$ ; the boundary points  $z_i$ ; the two central dots denote the AdS integrations; the straight lines are the standard bulk-to-bulk and bulk-to-boundary scalar propagators. On the right-hand side: each term in this sum is the 4-point scalar conformal block with specified intermediate conformal dimensions  $\tilde{h}$  and  $h_{ij|n} = h_i + h_j + 2n$ , the  $c$ -coefficients are given in section 2.2.

AdS/CFT correspondence, where AdS Feynman diagrams with boundary points known as Witten diagrams calculate CFT correlation functions [1–3]. It follows that the large- $N$  CFT correlators admit a holographic expansion in terms of Witten diagrams, a representation that is directly related to the conformal block decomposition. For example, in the case of the Euclidean AdS<sub>2</sub>/CFT<sub>1</sub> correspondence, the 4-point exchange Witten diagram decomposed into conformal blocks is shown in fig. 1.

In this paper, we focus on AdS Feynman diagrams which have all their endpoints in the bulk, i.e. those which are composed from the bulk-to-bulk propagators only, and argue that these diagrams have a similar decomposition in terms of Wilson line networks.<sup>1</sup> More precisely, one considers Feynman diagrams of scalar fields in two-dimensional Euclidean AdS space and shows that they can be decomposed into infinite sums of particular matrix elements of Wilson line networks stretched in the same space. Wilson line networks averaged between particular states are purely group-theoretical objects obtained by multiplying Wilson line operators in AdS and 3-valent intertwiners (i.e. 3-j Wigner symbols) and in this respect they are pretty similar to conformal blocks in CFT.<sup>2</sup>

Our basic example is the 3-point AdS Feynman diagram shown in fig. 2. This decomposition closely resembles the conformal block expansion of Witten diagrams. While the 3-point AdS Feynman diagram recovers the 3-point conformal correlation function on the boundary, its bulk structure reveals a series of terms remarkably similar to those of the 4-point Witten diagram. Specifically, it comprises a “single-trace” term and infinite sums of “double-trace” terms. Furthermore, it is noteworthy that the 2-point AdS Feynman diagram – representing the bulk-to-bulk scalar propagator – is equivalent to the 2-point Wilson line network (i.e., an ordinary Wilson line in AdS space) [18, 29].

There are two key points of our construction. The first one is that the HKLL holographic

<sup>1</sup>Wilson lines and their networks have many interesting properties, e.g. in the context of the AdS/CFT correspondence [4–27]: near the conformal boundary they reproduce conformal blocks, in the bulk they are probes of the background geometry.

<sup>2</sup>Recall that conformal blocks can be defined by averaging a particular combination of 3-valent intertwiners (this defines a channel) between primary states [28].

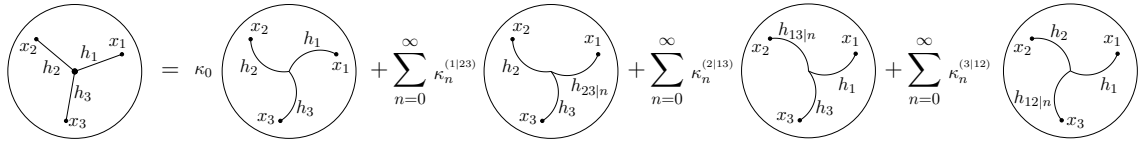


**Figure 2.** The Wilson line network decomposition of the 3-point  $\text{AdS}_2$  Feynman diagram. On the left-hand side: there are three scalars of masses  $m_i^2 = h_i(h_i - 1)$  located in the bulk points  $x_i$ ,  $i = 1, 2, 3$ ; the central dot denotes the AdS integration; the straight lines are the standard bulk-to-bulk scalar propagators. On the right-hand side: 3-valent graphs denote matrix elements of Wilson line networks which are Wilson lines (wavy lines) of three different weights connected by  $sl(2, \mathbb{R})$  intertwiners; weights  $h_{ij|n} = h_i + h_j + 2n$ , the  $\kappa$ -coefficients are given in section 4.1.

reconstruction [30–33] maps one-to-one  $n$ -point conformal blocks on the boundary onto Wilson network matrix elements with  $n$  endpoints in the bulk [29].<sup>3</sup> This is the general statement, although here we restrict ourselves to the 3-point case. We show that the 3-point Wilson network matrix element can be represented as an AdS integral involving a contour integration of the threefold product of appropriately modified bulk-to-bulk propagators. This integral representation stems directly from the HKLL reconstruction formula. The second one is the use of particular AdS propagator identities which allow one to transform the original AdS Feynman diagram into an infinite sum of AdS integrals over the modified bulk-to-bulk propagators, each of which is the Wilson network matrix element of particular conformal weights. The derivation and analysis of these propagator identities is central in this paper.

In section 2 we briefly review the HKLL holographic reconstruction which is needed for relating conformal blocks and Wilson line networks, here we introduce our conventions and notation. We also discuss the conformal block decomposition shown in fig. 1 as well as the AdS integral representation of conformal blocks in terms of geodesic Witten diagrams obtained by applying specific propagator identities that involve the standard bulk-to-bulk(boundary) propagators. In section 3 we uplift the mentioned propagator identities to AdS space. Here, we list a number of AdS propagator identities which relate the standard bulk-to-bulk and modified bulk-to-bulk propagators, we provide motivation for their introduction and discuss their properties. In section 4 we introduce Wilson line networks and formulate several lemmas, which formalize the AdS propagator identities discussed in the previous section. Here, we show how using these identities one can decompose the 3-point AdS Feynman diagram into Wilson network matrix elements as shown in fig. 2. Finally, we conclude with some discussions and future directions in section 5. Appendix A considers the analytic continuation of the 3-point Witten diagrams to the complex plane in the case of general and special dimensions. Appendix B contains the proofs of lemmas formulated in section 4.

<sup>3</sup>The 4-point CFT correlation function with one of fields being HKLL reconstructed was considered in [34].

## 2 HKLL reconstruction and Witten diagrams

### 2.1 Reconstruction formula

The HKLL reconstruction formula for the  $\text{AdS}_{d+1}$  fields in terms of the boundary  $\text{CFT}_d$  operators was derived in a series of papers [30–33]. Below we give the Euclidean version of the reconstruction formula in the  $\text{AdS}_2/\text{CFT}_1$  case, as the AdS integrals converge without the  $\varepsilon$ -prescription required in the Lorentzian case. Namely, assuming the  $1/N$  expansion, the bulk reconstruction formula for the Euclidean  $\text{AdS}_2$  scalar fields  $\phi(\mathbf{x})$  of the mass  $m^2 = h(h-1)$  with  $\mathbf{x} = (u, z)$  reads

$$\begin{aligned} \phi(\mathbf{x}) = & \int_{\mathcal{C}} dw \mathbb{K}_h(\mathbf{x}, w) \mathcal{O}_h(w) + \\ & + \frac{1}{N} \sum_{k,l=0}^{\infty} \sum_{n=0}^{\infty} \frac{a(h; h_k, h_l; n)}{\beta_{hh_kh_l}} \int_{\mathcal{C}} dw \mathbb{K}_{h_{kl|n}}(\mathbf{x}, w) \mathcal{O}_{h_{kl|n}}(w) + O\left(\frac{1}{N^2}\right). \end{aligned} \quad (2.1)$$

1. The Poincare patch of the Euclidean  $\text{AdS}_2$  in the local coordinates  $\mathbf{x}$  has the metric

$$ds^2 = \frac{dz^2 + du^2}{u^2}, \quad u \in \mathbb{R}_{\geq 0}, z \in \mathbb{R}. \quad (2.2)$$

The conformal boundary of the global  $\text{AdS}_2$  is disconnected. Here, we choose one connected component, which we denote as  $\partial\text{AdS}_2$ . It is placed at  $u = 0$ . Also, the metric determinant  $g(\mathbf{x}) = 1/u^4$ .

2.  $\mathcal{C}$  is a line contour between the points  $z \pm iu$  on the complexified conformal boundary, which is the standard complex plane,  $(\partial\text{AdS}_2)^{\mathbb{C}} \cong \mathbb{C}$ . The integration contour  $\mathcal{C}$  is the Wick rotated integration contour  $\mathcal{C}_{\text{Lor}}$  of the Lorentzian HKLL integral, where  $\mathcal{C}_{\text{Lor}} = [z - u, z + u]$  is the line segment on  $\mathbb{R}$ . It has a simple geometric interpretation:  $\mathcal{C}_{\text{Lor}}$  consists of boundary points which are spacelike separated from the bulk point  $(u, z)$  in the Lorentzian  $\text{AdS}_2$ . It follows that in the Euclidean HKLL integral formula (2.1) we deal with functions analytically continued on the complex plane,  $w \in \mathbb{C}$ .
3.  $\mathbb{K}_h(\mathbf{x}, w)$  is the smearing function, which is the bulk-to-boundary propagator of dual conformal weight  $1 - h$ :

$$\mathbb{K}_h(\mathbf{x}, w) = \frac{-2i}{4^h} \frac{\Gamma(2h)}{\Gamma(h)\Gamma(h)} \left( \frac{u}{u^2 + (z - w)^2} \right)^{1-h}. \quad (2.3)$$

Note that our definition of the smearing function slightly differs from that in [30]. The original HKLL formula integrates over the entire conformal boundary, and its smearing function uses Heaviside step functions to restrict the integration domain to the line contour  $\mathcal{C}_{\text{Lor}}$ . Since the integration contour  $\mathcal{C}$  in the Euclidean version is complex, it is more convenient to resolve Heaviside step functions so that the smearing function is given by (2.3).

4.  $\mathcal{O}_h(w)$  is a primary field of conformal weight  $h$ .  $\mathcal{O}_{h_{kl|n}}(w)$  are double-trace fields built of two primary fields  $\mathcal{O}_{h_k}$  and  $\mathcal{O}_{h_l}$  as

$$\mathcal{O}_{h_{kl|n}}(w) = \sum_{i=0}^{2n} c_i(h_k, h_l, n) \partial^i \mathcal{O}_{h_k}(w) \partial^{2n-i} \mathcal{O}_{h_l}(w), \quad (2.4)$$

where coefficients  $c_i(h_k, h_l, n)$  can be chosen so that the double-trace field is primary of conformal weight  $h_{kl|n} = h_k + h_l + 2n$ . The sum over  $k$  and  $l$  on the right-hand side of (2.1) goes over all primary fields in a boundary CFT.

5. The coefficients  $\beta_{hh_kh_l}$  are the 3-point structure constants in CFT. The coefficients  $a(h; h_k, h_l; n)$  (in the  $d = 1$  case) are given by

$$a(h; h_k, h_l; n) = \frac{2\pi^{\frac{1}{2}}}{\Gamma(h)} \frac{(-)^n (h_k)_n (h_l)_n}{n! (h_k + h_l - \frac{1}{2} + n)_n} \frac{\Gamma(h + \frac{1}{2})}{h(h-1) - (h_{kl|n})(h_{kl|n} - 1)}, \quad (2.5)$$

where  $(a)_n = \Gamma(a+n)/\Gamma(a)$  is the Pochhammer symbol. They are fixed by analyticity of the bulk-to-boundary correlation functions  $\langle \phi(\mathbf{x}) \mathcal{O}_{h_k}(w_2) \mathcal{O}_{h_l}(w_3) \rangle$  [30–33].

The reconstruction formula (2.1) implies that the corresponding reconstruction relations between correlation functions of the bulk fields  $\phi(\mathbf{x})$  and correlation functions of the primary fields  $\mathcal{O}_h(z)$  are represented in terms of multiple integrals of the boundary correlation functions which can be expanded in conformal blocks. In general, such relations can be quite complicated. Near the conformal boundary, they are, however, simple: the extrapolate dictionary relation equates the bulk correlation functions at  $u \rightarrow 0$  with the boundary conformal correlation functions [35]. This can be directly seen from the reconstruction formula (2.1): at  $u \rightarrow 0$  the integration contour  $\mathcal{C}$  shrinks to the boundary point  $z$  that removes the integration; then, one shows that the second term is sub-leading, whereas the leading term is proportional to the primary field, thereby producing the asymptotic value  $\phi(\mathbf{x}) \simeq u^h \mathcal{O}_h(z)$ .

## 2.2 Conformal block decomposition

Any bulk correlation function can be decomposed into AdS Feynman diagrams comprising multiple integrals over AdS space, where the integrands are products of bulk-to-bulk propagators. For a given diagram with all points on the boundary the resulting expression can be explicitly obtained as a sum of conformal blocks, where intermediate channels correspond to single-trace and double-trace exchange fields inherited from the reconstruction formula (2.1) (note that at  $O(1/N^2)$  only tree-level diagrams contribute). The example of the 4-point exchange Witten diagram in  $\text{AdS}_2$  space reads (see fig. 3) [36]<sup>4</sup>

$$\begin{aligned} & \iint_{\text{AdS}_2} d^2 \mathbf{x} d^2 \mathbf{x}' \sqrt{g(\mathbf{x})g(\mathbf{x}')} K_{h_1}(\mathbf{x}, z_1) K_{h_2}(\mathbf{x}, z_2) G_{\tilde{h}}(\mathbf{x}, \mathbf{x}') K_{h_3}(\mathbf{x}', z_3) K_{h_4}(\mathbf{x}', z_4) = \\ & = c_0 F_{h\tilde{h}}(z_1, \dots, z_4) + \sum_{n=0}^{\infty} c_n^{(12|34)} F_{hh_{12|n}}(z_1, \dots, z_4) + \sum_{n=0}^{\infty} c_n^{(34|12)} F_{hh_{34|n}}(z_1, \dots, z_4), \end{aligned} \quad (2.6)$$

<sup>4</sup>The 4-point exchange Witten diagram was calculated in [37, 38]. The corresponding conformal block decomposition was found in [39–41]. The 4-point contact Witten diagram has the similar representation [36].

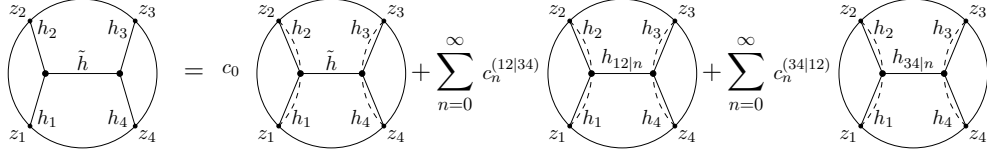


**Figure 3.** The exchange Witten diagram (2.6) of four scalars of mass  $m_i^2 = h_i(h_i - 1)$  and one exchange scalar of mass  $\tilde{m}^2 = \tilde{h}(\tilde{h} - 1)$ . The conformal boundary  $\partial\text{AdS}_2$  is shown by the circle, the two bulk points are  $\mathbf{x}$  and  $\mathbf{x}'$ . Each term in this decomposition is a geodesic Witten diagram obtained by restricting the integration domain of the exchange Witten diagram to geodesics (dashed lines) connecting boundary points  $z_1, z_2$  and  $z_3, z_4$ . Each geodesic Witten diagram computes the conformal block with particular intermediate conformal weight [36].

where  $G_h(\mathbf{x}, \mathbf{x}')$  is the bulk-to-bulk propagator of a scalar field of mass  $m^2 = h(h - 1)$  [42]

$$G_h(\mathbf{x}, \mathbf{x}') = \left( \frac{\xi(\mathbf{x}, \mathbf{x}')}{2} \right)^h {}_2F_1 \left[ \frac{h}{2}, \frac{h}{2} + \frac{1}{2}; h + \frac{1}{2} \mid \xi(\mathbf{x}, \mathbf{x}')^2 \right], \quad \xi(\mathbf{x}, \mathbf{x}') = \frac{2uu'}{u^2 + u'^2 + (z - z')^2}; \quad (2.7)$$

the bulk-to-boundary propagator  $K_h(\mathbf{x}, z')$  is obtained by taking one of the bulk points to the conformal boundary

$$K_h(\mathbf{x}, z') = \left( \frac{u}{u^2 + (z - z')^2} \right)^h, \quad (2.8)$$

cf. (2.3); the functions  $F_{hh'}(z_1, \dots, z_4)$  are the 4-point scalar conformal blocks with external dimensions  $h_1, \dots, h_4$  and intermediate dimensions  $h' = \tilde{h}$  or  $h' = h_{ij|n} = h_i + h_j + 2n$ , and

$$c_0 = \beta_{h_1 h_2 \tilde{h}} \beta_{\tilde{h} h_3 h_4} \sum_{m,n=0}^{\infty} \frac{a(\tilde{h}; h_1, h_2; m)}{\beta_{h_{12|m} h_1 h_2}} \frac{a(\tilde{h}; h_3, h_4; n)}{\beta_{h_{34|n} h_3 h_4}}, \quad (2.9)$$

$$c_n^{(ij|kl)} = a(\tilde{h}; h_i, h_j; n) \beta_{h_{ij|n} h_k h_l} \sum_{m=0}^{\infty} \frac{a(h_{ij|n}; h_k, h_l; m)}{\beta_{h_{kl|m} h_k h_l}},$$

where the  $a$ -coefficients are given by (2.5). It is worth noting that the  $a$ -coefficients arise in two different calculations: the HKLL reconstruction and the tree-level Witten diagram decomposition into conformal blocks, the relation between which has not been directly studied in the literature.

There are three crucial steps in deriving the decomposition (2.6) [36, 43]. Firstly, the infinite sum over single-trace and double-trace terms on the right-hand side is directly obtained by using particular propagator identities applied to the bulk-to-bulk and bulk-to-boundary propagators in the integrand on the left-hand side. In particular, the identity producing the

infinite sum on the right-hand side of (2.6) is given by<sup>5</sup>

$$\begin{aligned} \int_{\text{AdS}_2} d^2 \mathbf{x} \sqrt{g(\mathbf{x})} K_{h_1}(\mathbf{x}, z_1) K_{h_2}(\mathbf{x}, z_2) f(\mathbf{x}) &= \sum_{n=0}^{\infty} \frac{1}{\beta_{h_{12|n} h_1 h_2}} \frac{(-)^n (h_1)_n (h_2)_n}{n! (h_1 + h_2 + n - \frac{1}{2})_n} \\ &\times \int_{\gamma_{12}} d\lambda \int_{\text{AdS}_2} d^2 \mathbf{x} \sqrt{g(\mathbf{x})} K_{h_1}(\mathbf{x}(\lambda), z_1) K_{h_2}(\mathbf{x}(\lambda), z_2) G_{h_{12|n}}(\mathbf{x}(\lambda), \mathbf{x}) f(\mathbf{x}), \end{aligned} \quad (2.10)$$

where  $f(\mathbf{x})$  is a test function and  $\gamma_{12}$  is a geodesic  $\mathbf{x} = \mathbf{x}(\lambda)$  connecting two boundary points  $z_1$  and  $z_2$ . Secondly, each term in the resulting infinite sum is given by the so-called geodesic Witten diagram, see fig. 3. These diagrams have the same topology as the original diagram but now the integrals are taken over the geodesics instead of  $\text{AdS}_2$ :

$$\iint_{\text{AdS}_2} d^2 \mathbf{x} d^2 \mathbf{x}' \sqrt{g(\mathbf{x})g(\mathbf{x}')} \rightarrow \int_{\gamma_{12}} d\lambda \int_{\gamma_{34}} d\lambda'. \quad (2.11)$$

Thirdly, the geodesic Witten diagram computes the conformal block. In other words, the conformal block being a part of the conformal correlation function has its own AdS integral representation.<sup>6</sup>

This method was applied to expand the 5-point and 6-point contact and exchange Witten diagrams in different channels [52, 53]. While the 6-point conformal block in the snowflake channel has a simple AdS representation, which directly generalizes the 4-point case, a similar expression for the 5-point conformal block in the comb channel is more intricate.<sup>7</sup> This is due to the fact that the procedure of constructing a geodesic Witten diagram requires vertices to have only an even number of bulk-to-boundary propagators, whereas a Witten diagram with an odd number of boundary points does not meet this requirement.

### 3 AdS integral identities and modified propagators

The decomposition method described in the previous section applies to Witten diagrams, i.e. to AdS Feynman diagrams with boundary endpoints only. In order to have an expansion into single-trace and double-trace terms for AdS Feynman diagrams in the bulk (i.e. such functions which reproduce the conformal block decomposition (2.6) when restricted on the boundary) one needs to have a bulk version of the propagator identities of the type (2.10). In this paper, we show that in the 3-point case this can be achieved by using three integral identities valid in Euclidean  $\text{AdS}_2$  space. Note that the AdS integrals in the Poincare coordinates (2.2) are given by

$$\int_{\mathbb{D}_0} d^2 \mathbf{x} \sqrt{g(\mathbf{x})} \rightarrow \int_{\mathbb{D}_1} \frac{du}{u^2} \int_{\mathbb{D}_2} dz, \quad (3.1)$$

---

<sup>5</sup>Here we integrated the identity from [36] with a test function.

<sup>6</sup>Geodesic Witten diagrams in  $\text{AdS}_d$  were extensively studied from many perspectives, see e.g. [44–53]. The analogous construction exists in  $\text{AdS}_3$ , where the large- $c$  Virasoro conformal blocks are represented by lengths of geodesic networks, see e.g. [6, 43, 44, 54–62].

<sup>7</sup>The 4-point and 5-point conformal blocks exist only in the comb channel. The 6-point conformal blocks can also exist in the snowflake channel.

where  $\mathbb{D}_{0,1,2}$  are some integration domains. The  $z$ -variable in the integral identities given below is extended to the complex plane, yielding particular integration contours that encircle the resulting poles of the integrands. Depending on whether  $\mathbb{D}_0$  has compact dimensions, the domains  $\mathbb{D}_{1,2}$  can be compact or not.

### 3.1 Three identities

- The conversion identity:

$$G_h(\mathbf{x}, \mathbf{x}') = \int_{z'-iu'}^{z'+iu'} dw \widehat{G}_h(\mathbf{x}, \mathbf{x}', w). \quad (3.2)$$

- The superposition identity:

$$\begin{aligned} \int_{\text{AdS}_2} d^2\mathbf{x} \sqrt{g(\mathbf{x})} G_h(\mathbf{x}, \mathbf{x}') f(\mathbf{x}) &= \int_{z'-iu'}^{z'+iu'} dw \int_0^\infty \frac{du}{u^2} \int_C dz \widehat{G}_h(\mathbf{x}, \mathbf{x}', w) f(\mathbf{x}) + \\ &+ \pi \int_0^{u'} \frac{du}{u^2} \int_{z'-i(u-u')}^{z'+i(u-u')} dz \widetilde{G}_h(\mathbf{x}, \mathbf{x}') f(\mathbf{x}). \end{aligned} \quad (3.3)$$

- The splitting identity:

$$\begin{aligned} \int_0^{u_3} \frac{du}{u^2} \int_{z_3-i(u-u_3)}^{z_3+i(u-u_3)} dz G_{h_1}(\mathbf{x}, \mathbf{x}_1) G_{h_2}(\mathbf{x}, \mathbf{x}_2) \widetilde{G}_{h_3}(\mathbf{x}, \mathbf{x}_3) &= \\ = \sum_{n=0}^{\infty} \frac{a(h_3; h_1, h_2; n)}{\rho_{h_1, h_2, n}} \int_{z_3-iu_3}^{z_3+iu_3} dw \oint_0 \frac{du}{u^2} \oint_P dz G_{h_1}(\mathbf{x}, \mathbf{x}_1) G_{h_2}(\mathbf{x}, \mathbf{x}_2) \widehat{G}_{h_{12|n}}(\mathbf{x}, \mathbf{x}_3, w). \end{aligned} \quad (3.4)$$

Here, the bulk coordinates are  $\mathbf{x} = (u, z)$ ,  $\mathbf{x}' = (u', z')$ ,  $f(\mathbf{x})$  is a test function,  $\rho_{h_1, h_2, n}$  is some coefficient, and

$$\begin{aligned} \widehat{G}_h(\mathbf{x}, \mathbf{x}', w) &= K_h(\mathbf{x}, w) \mathbb{K}_h(\mathbf{x}', w), \\ \widetilde{G}_h(\mathbf{x}, \mathbf{x}') &= \frac{-2i}{4^h} \frac{\Gamma(2h)}{\Gamma(h)\Gamma(h)} \left( \frac{\Gamma(1-2h)}{\Gamma(1-h)^2} G_h(\mathbf{x}, \mathbf{x}') + \frac{\Gamma(2h-1)}{\Gamma(h)^2} G_{1-h}(\mathbf{x}, \mathbf{x}') \right). \end{aligned} \quad (3.5)$$

Functions  $\widehat{G}_h$  and  $\widetilde{G}_h$  were originally introduced in [31] as propagators in Lorentzian  $\text{AdS}_2$  space (see our discussion in section 3.3). They are solutions of the homogeneous Klein-Gordon (KG) equation. Note that  $\widehat{G}_h = \widehat{G}_h(\mathbf{x}(u, z), \mathbf{x}'(u', z'), w)$  arising in (3.2)–(3.4) is analytically continued on the complex  $z$ -plane, where it has poles at  $z = w \pm iu$ ,  $w \in \mathbb{C}$ ,  $u \in \mathbb{R}$ . The corresponding integration contours  $C$  and  $P$  on the complex plane are shown in fig. 4. A detailed discussion of the above identities will be given in section 4.

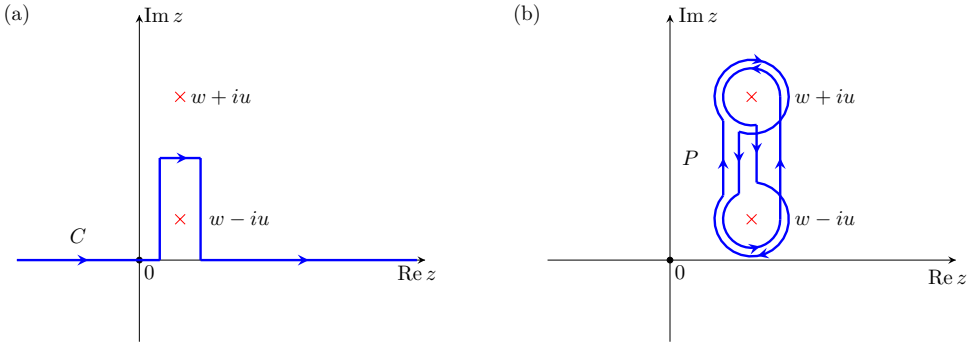


**Figure 4.** (a) The contour  $C$  on the complex  $z$ -plane  $\mathbb{C}$ . The red crosses are poles of the analytically continued propagator  $\widehat{G}_h(\mathbf{x}(u, z), \mathbf{x}'(u', z'), w)$ . (b) The Pochhammer contour  $P$  in  $\mathbb{C} \setminus \{w - iu, w + iu\}$ .

### 3.2 Modified AdS Feynman diagrams

Using the two modified propagators (3.5) instead of the standard ones results in modified AdS Feynman diagrammatics. Several useful properties highlight different roles of  $\widehat{G}$  and  $\widetilde{G}$ . Simultaneously, the integral identities allow one to decompose standard AdS Feynman diagrams into infinite sums of modified AdS Feynman diagrams.

**Decomposition.** Let us consider the 3-point AdS Feynman diagram, which we schematically write as  $\int GGG$ . One applies the identities (3.2)–(3.4) in four steps.

1. Apply the superposition identity (3.3) to any  $G$  inside the AdS Feynman diagram. The result is the sum of two terms:  $\int GGG \rightarrow \int \widehat{G}GG + \int \widetilde{G}GG$ .
2. Repeat this step in the first term  $\int \widehat{G}GG$  for another  $G$  until no  $G$  are left. The term without  $\widetilde{G}$  is the single-trace contribution.
3. Replace each  $G$  in the every term by  $\widehat{G}$  using the conversion identity (3.2).
4. Convert each term with  $\widetilde{G}$  into the term with  $\widehat{G}$  by means of the splitting identity (3.4). This produces an infinite sum of double-trace contributions.

Here and below, the terminology *single-trace* and *double-trace* is used in the following sense. A contribution is considered single-trace if the modified propagators in an AdS Feynman diagram have weights that are not composites of the original  $h_i$  ( $i = 1, 2, 3$ ). Conversely, a contribution is considered as double-trace if at least one of the modified propagators has a composite weight  $h_{ij|n} = h_i + h_j + 2n$  ( $n = 0, 1, 2, \dots$ ).

Schematically, the above algorithm can be represented as follows:

$$\begin{aligned}
\int G_1 G_2 G_3 &\xrightarrow{(3.3)} \int \color{blue}{\widehat{G}_1} G_2 G_3 + \int \color{red}{\widetilde{G}_1} G_2 G_3 \xrightarrow{(3.3)} \int \color{blue}{\widehat{G}_1} \color{blue}{\widehat{G}_2} G_3 + \int \color{red}{\widetilde{G}_1} G_2 G_3 + \int \color{blue}{\widehat{G}_1} \color{red}{\widetilde{G}_2} G_3 \\
&\xrightarrow{(3.3), (3.2)} \int \color{blue}{\widehat{G}_1} \color{blue}{\widehat{G}_2} \color{blue}{\widehat{G}_3} + \int \color{red}{\widetilde{G}_1} \color{blue}{\widehat{G}_2} \color{blue}{\widehat{G}_3} + \int \color{blue}{\widehat{G}_1} \color{red}{\widetilde{G}_2} \color{blue}{\widehat{G}_3} + \int \color{blue}{\widehat{G}_1} \color{blue}{\widehat{G}_2} \color{red}{\widetilde{G}_3} \\
&\xrightarrow{(3.4)} \underbrace{\int \color{blue}{\widehat{G}_1} \color{blue}{\widehat{G}_2} \color{blue}{\widehat{G}_3}}_{\text{single-trace}} + \underbrace{\left( \sum_n a_n^{23} \int \color{blue}{\widehat{G}_{23|n}} \color{blue}{\widehat{G}_2} \color{blue}{\widehat{G}_3} + (1 \leftrightarrow 2) + (1 \leftrightarrow 3) \right)}_{\text{double-trace}}, \tag{3.6}
\end{aligned}$$

where  $a_n^{23}$  are fixed coefficients and  $G_i = G_{h_i}(\mathbf{x}, \mathbf{x}_i)$ ,  $G_{ij|n} = G_{h_{ij|n}}(\mathbf{x}, \mathbf{x}_k)$ ,  $i \neq j \neq k \neq i$ .

Note that we obtained the second line in (3.6) only by means of the conversion and superposition identities:

$$\int G_1 G_2 G_3 = \int \color{blue}{\widehat{G}_1} \color{blue}{\widehat{G}_2} \color{blue}{\widehat{G}_3} + \int \color{red}{\widetilde{G}_1} \color{blue}{\widehat{G}_2} \color{blue}{\widehat{G}_3} + \int \color{blue}{\widehat{G}_1} \color{red}{\widetilde{G}_2} \color{blue}{\widehat{G}_3} + \int \color{blue}{\widehat{G}_1} \color{blue}{\widehat{G}_2} \color{red}{\widetilde{G}_3}. \tag{3.7}$$

**Equations of motion.** Let us act with the KG operators  $\square_{\mathbf{x}_i} - h_i(h_i - 1)$ , where  $\square_{\mathbf{x}_i}$  is the Laplace-Beltrami operator in local coordinates  $\mathbf{x}_i \in \text{AdS}_2$ , to each term on the right-hand side of the decomposition (3.7):

$$(\square_{\mathbf{x}_i} - h_i(h_i - 1)) \int \color{blue}{\widehat{G}_1} \color{blue}{\widehat{G}_2} \color{blue}{\widehat{G}_3} = 0, \quad i = 1, 2, 3; \tag{3.8}$$

$$(\square_{\mathbf{x}_i} - h_i(h_i - 1)) \int \color{red}{\widetilde{G}_i} \color{blue}{\widehat{G}_j} \color{blue}{\widehat{G}_k} = -\delta_{il} \frac{2\sqrt{\pi} \Gamma(h_i + \frac{1}{2})}{\Gamma(h_i)} G_{h_j}(\mathbf{x}_j, \mathbf{x}_i) G_{h_k}(\mathbf{x}_k, \mathbf{x}_i), \quad i \neq j \neq k \neq i,$$

where  $\delta_{il}$  is the Kronecker symbol. We conclude that terms that contain the propagator  $\color{red}{\widetilde{G}_i}(\mathbf{x}, \mathbf{x}_i)$  satisfy the inhomogeneous KG equation in  $\mathbf{x}_i$  and the homogeneous KG equation in  $\mathbf{x}_j \neq \mathbf{x}_i$ , whereas terms which do not contain this propagator satisfy the homogeneous KG equations. In other words, the presence or absence of  $\color{red}{\widetilde{G}_i}(\mathbf{x}, \mathbf{x}_i)$  completely defines how the KG operators act on the modified AdS Feynman diagram. Similarly, the modified AdS Feynman diagram containing the propagator  $\color{blue}{\widehat{G}_i}(\mathbf{x}, \mathbf{x}_i, w_i)$  satisfies the homogeneous KG equation in  $\mathbf{x}_i$ .

**Boundary asymptotics.** By direct calculation one shows that the leading asymptotics ( $u_i \rightarrow 0$ ) in the decomposition (3.7) are given by

$$\begin{aligned}
\int \color{blue}{\widehat{G}_1} \color{blue}{\widehat{G}_2} \color{blue}{\widehat{G}_3} &= \prod_{k=1}^3 \int_{z_k + iu_k}^{z_k - iu_k} dw_k \int_0^\infty \frac{du}{u^2} \int_C dz \prod_{m=1}^3 \color{blue}{\widehat{G}_{h_m}}(\mathbf{x}, \mathbf{x}_m, w_m) \\
&\xrightarrow{u_{1,2,3} \rightarrow 0} u_1^{h_1} u_2^{h_2} u_3^{h_3} \int_0^\infty \frac{du}{u^2} \int_{\mathbb{R}} dz K_{h_1}(\mathbf{x}, z_1) K_{h_2}(\mathbf{x}, z_2) K_{h_3}(\mathbf{x}, z_3), \tag{3.9}
\end{aligned}$$

$$\int \tilde{G}_i \tilde{G}_j \tilde{G}_k = \prod_{m=j,k} \int_{z_m + iu_m}^{z_m - iu_m} dw_m \int_0^{u_i} \frac{du}{u^2} \int_{z_i - i(u-u_i)}^{z_i + i(u-u_i)} dz \tilde{G}_{h_i}(\mathbf{x}, \mathbf{x}_i) \tilde{G}_{h_j}(\mathbf{x}, \mathbf{x}_j, w_j) \tilde{G}_{h_k}(\mathbf{x}, \mathbf{x}_k, w_k) \\ \stackrel{u_{1,2,3} \rightarrow 0}{\simeq} \eta u_i^{h_j+h_k} u_j^{h_j} u_k^{h_k} \oint_0^{\frac{du}{u^2}} \oint_{P[z_i - iu, z_i + iu]} dz K_{h_j+h_k}(\mathbf{x}, z_i) K_{h_j}(\mathbf{x}, z_j) K_{h_k}(\mathbf{x}, z_k),$$

where  $\eta$  is some coefficient, the contour  $C$  is shown in fig. 5. The mnemonic rule here is that, near the boundary, the bulk-to-boundary propagator  $u_i^{h_i} K_{h_i}(\mathbf{x}, z_i)$  (2.8) corresponds to the modified propagator  $\tilde{G}_{h_i}(\mathbf{x}, \mathbf{x}_i, w_i)$ , whereas the propagator  $u_i^{h_j+h_k} K_{h_j+h_k}(\mathbf{x}, z_i)$  corresponds to the modified propagator  $\tilde{G}_{h_i}(\mathbf{x}, \mathbf{x}_i)$ , with  $i \neq j \neq k \neq i$ . This correspondence is valid only in the context of the modified 3-point AdS Feynman diagrams, because the near-boundary behavior of standard and modified propagators differs. Specifically, the integration domains of modified diagrams depend on  $u_i$ , which directly modifies their asymptotic behavior near the boundary.

Now, substituting the above asymptotic relations into (3.7) one obtains (schematically)

$$u_1^{h_1} u_2^{h_2} u_3^{h_3} \int K_1 K_2 K_3 \simeq u_1^{h_1} u_2^{h_2} u_3^{h_3} \int K_1 K_2 K_3 + u_1^{h_2+h_3} u_2^{h_2} u_3^{h_3} \int K_{2+3} K_2 K_3 \\ + u_1^{h_1} u_2^{h_1+h_3} u_3^{h_3} \int K_1 K_{1+3} K_3 + u_1^{h_1} u_2^{h_2} u_3^{h_1+h_2} \int K_1 K_2 K_{1+2}, \quad (3.10)$$

where we simplified our notation for integrals and denoted the bulk-to-boundary propagators as  $K_i \equiv K_{h_i}(\mathbf{x}, z_i)$ ,  $K_{j+k} \equiv K_{h_j+h_k}(\mathbf{x}, z_i)$ ,  $i \neq j \neq k \neq i$ . The first term on the right-hand side has the same leading behavior as the left-hand side. Note that the other three terms are sub-leading if the weights  $h_i$  are subject to the triangle inequalities

$$h_1 < h_2 + h_3, \quad h_2 < h_1 + h_3, \quad h_3 < h_1 + h_2, \quad (3.11)$$

otherwise the relation (3.10) is incorrect. This reflects the fact that the 3-point Witten diagram on the left-hand side of (3.10) diverges when the triangle inequalities are not satisfied. The three sub-leading terms come from the modified diagrams containing  $\tilde{G}_{h_i}$ , which correspond to the double-trace terms according to the decomposition (3.6). In other words, the double-trace terms near the boundary fall off faster than the single-trace term provided that the triangle inequalities are satisfied.

**Contact diagrams.** As the superposition identity (3.3) is formulated with a test function  $f(\mathbf{x})$ , one can expand the  $n$ -point *contact* AdS Feynman diagram into modified diagrams by choosing a test function to be a product of  $n-1$  bulk-to-bulk propagators. Then, applying the superposition identity  $n$  times one obtains

$$\int \prod_{i=1}^n G_i = \int \prod_{i=1}^n \tilde{G}_i + \int \tilde{G}_1 \prod_{i=2}^n \tilde{G}_i + \int \tilde{G}_2 \prod_{\substack{i=1 \\ i \neq 2}}^n \tilde{G}_i + \dots + \int \tilde{G}_n \prod_{i=1}^{n-1} \tilde{G}_i, \quad (3.12)$$

where we also used the conversion identity (3.2) to replace every  $G$  on the right-hand side by  $\tilde{G}$ . Note that the action of the KG operators on (3.12) yields a set of relations similar to (3.8). The roles of the modified propagators  $\tilde{G}$  and  $\tilde{G}$  in the  $n$ -point case remain the same.

The near-boundary ( $u_i \rightarrow 0$ ) asymptotic expansion of (3.12) is given by

$$\prod_{i=1}^n u_i^{h_i} \int \prod_{j=1}^n K_j \simeq \prod_{i=1}^n u_i^{h_i} \int \prod_{j=1}^n K_j + \sum_{k=1}^n \prod_{\substack{i=1 \\ i \neq k}}^n (u_k u_i)^{h_i} \int K_{1+\dots+\cancel{k}+\dots+n} \prod_{\substack{j=1 \\ j \neq k}}^n K_j, \quad (3.13)$$

where we defined  $K_{1+\dots+\cancel{k}+\dots+n} \equiv K_{h_1+\dots+\cancel{h_k}+\dots+h_n}(\mathbf{x}, z_k)$  and taken only the leading asymptotics of each term. The analysis of (3.13) is essentially the same as in the 3-point case, the only difference is that in the  $n$ -point case the propagator  $\tilde{G}_{h_k}(\mathbf{x}, \mathbf{x}_k)$  corresponds to the bulk-to-boundary propagator  $u_k^{h_1+\dots+\cancel{h_k}+\dots+h_n} K_{1+\dots+\cancel{k}+\dots+n}$ . Also note that the first term in (3.13) is leading only if the weights are subject to the generalized triangle inequalities

$$h_1 + \dots - h_k + \dots + h_n \geq 0, \quad \forall k \in \{1, \dots, n\}. \quad (3.14)$$

### 3.3 Commentary

Firstly, we note that the identities (3.2) and (3.3) have much in common with an identity relating the bulk-to-bulk and modified propagators defined in Lorentzian  $\text{AdS}_2$  space [31]:

$$G_h(\mathbf{x}, \mathbf{x}') = \pi \theta(u' - u) \theta(u' - u - |z' - z|) \tilde{G}_h(\mathbf{x}, \mathbf{x}') + i \int_{z' - u'}^{z' + u'} dw \hat{G}_h(\mathbf{x}, \mathbf{x}', w), \quad (3.15)$$

where  $\theta(x)$  is the Heaviside step function. Consider the conversion identity (3.2). In a domain where the step functions vanish, (3.15) is a special case of (3.2). On the other hand, the identity (3.15) can be integrated over  $\text{AdS}_2$  space using a test function and subsequently subjected to the Wick rotation. One can show that the result is given by the superposition identity (3.3), provided a specific class of test functions is chosen. See our discussion around (B.47) in Appendix B.4.

Secondly, the superposition identity (3.3) can be applied to any AdS Feynman diagram; specifically, a test function  $f(\mathbf{x})$  can be chosen as a product of any number of propagators. On the other hand, the splitting identity (3.4) transforms the product of only three bulk-to-bulk propagators, therefore, it can be applied only when an AdS Feynman diagram has at least one 3-valent vertex. The splitting identity can be seen as a direct analogue of the propagator identity (2.10) in the sense that both identities produce infinite sums of double-trace terms and add one-dimensional integration (i.e. a number of integrations on the left and right differs by one).

Thirdly, we note that the single-trace contribution is directly obtained by replacing each bulk-to-bulk propagators  $G$  by the modified propagator  $\hat{G}$ , see the last line in (3.6). In the context of 2d thermal conformal correlators this trick was proposed in [63]. The authors changed the bulk-to-bulk propagator inside the 2-point Witten diagram in the thermal  $\text{AdS}_3$  as

$$G_h(x_1, x_2) \longrightarrow \int_{\partial \text{AdS}_3} dz d\bar{z} \hat{G}_h(x_1, x_2; z, \bar{z}), \quad (3.16)$$

where the conformal boundary  $\partial \text{AdS}_3 \cong \mathbb{T}^2$ . The integrand is the  $\text{AdS}_3$  version of the modified propagator  $\hat{G}_h(\mathbf{x}, \mathbf{x}', w)$  (3.5). This propagator contains the Heaviside step functions

restricting the integration domain like in the standard formulation of the HKLL reconstruction (see the discussion below (2.3)). The substitution (3.16) results in the modified Witten diagram which obeys the Casimir equation for the 2-point torus conformal block [63].

## 4 Wilson network decomposition of AdS Feynman diagrams

The purpose of this section is twofold. First, we rigorously derive the propagator identities discussed in the previous section. Second, we show that their application yields an infinite expansion of the 3-point  $\text{AdS}_2$  Feynman diagram with bulk endpoints, wherein each term corresponds to the 3-point Wilson line network in  $\text{AdS}_2$  space carrying the particular conformal weights.

### 4.1 Wilson networks as basis functions

Let us briefly recap what we mean by the Wilson line networks in  $\text{AdS}_2$  space, which has an isometry algebra  $sl(2, \mathbb{R})$  [27] (see also [8, 9, 16, 18, 23]). The 3-point Wilson line network is built by contracting 3-valent  $sl(2, \mathbb{R})$  intertwiner carrying external weights  $h_1, h_2, h_3$  with three Wilson line operators of weights  $h_1, h_2, h_3$  connecting the point  $\mathbf{x} = 0$  and the points  $\mathbf{x}_1, \mathbf{x}_2, \mathbf{x}_3$  in the bulk. Thus, this is an operator in the tensor product of three (infinite-dimensional)  $sl(2, \mathbb{R})$  Verma modules. Let  $\mathcal{V}_{h_1 h_2 h_3}(\mathbf{x}_1, \mathbf{x}_2, \mathbf{x}_3)$  be a particular matrix element of the Wilson line network, it is evaluated between three cap states which are the Ishibashi states. In what follows, we refer to these matrix elements as 3-point *AdS vertex functions*. The AdS vertex functions can be explicitly calculated as multivariate generalized hypergeometric series [29]. The  $n$ -point construction can be found in [27].

The crucial property of the  $n$ -point AdS vertex functions is that they are HKLL reconstructed  $n$ -point global conformal blocks in the comb channel [29] (see (4.4) below). Here, we keep the leading contribution of the  $1/N$  expansion, where the role of  $N$  is played by the large central charge. Therefore, the Virasoro conformal blocks with light operators ( $h = O(c^0)$ ) in the limit  $c \rightarrow \infty$  reduce to the global conformal blocks, which are  $sl(2, \mathbb{R})$  conformal blocks in this case.

The 3-point AdS Feynman diagram in the bulk can be expanded into the 3-point AdS vertex functions [29]:<sup>8</sup>

$$\begin{aligned} & \int_{\text{AdS}_2} d^2 \mathbf{x} \sqrt{g(\mathbf{x})} G_{h_1}(\mathbf{x}, \mathbf{x}_1) G_{h_2}(\mathbf{x}, \mathbf{x}_2) G_{h_3}(\mathbf{x}, \mathbf{x}_3) \\ &= \kappa_0 \mathcal{V}_{h_1 h_2 h_3}(\mathbf{x}_1, \mathbf{x}_2, \mathbf{x}_3) + \sum_{n=0}^{\infty} \kappa_n^{(1|23)} \mathcal{V}_{h_{23|n} h_2 h_3}(\mathbf{x}_1, \mathbf{x}_2, \mathbf{x}_3) \\ &+ \sum_{n=0}^{\infty} \kappa_n^{(2|13)} \mathcal{V}_{h_1 h_{13|n} h_3}(\mathbf{x}_1, \mathbf{x}_2, \mathbf{x}_3) + \sum_{n=0}^{\infty} \kappa_n^{(3|12)} \mathcal{V}_{h_1 h_2 h_{12|n}}(\mathbf{x}_1, \mathbf{x}_2, \mathbf{x}_3), \end{aligned} \quad (4.1)$$

---

<sup>8</sup>The 3-point AdS Feynman diagram with two boundary points was calculated in [64], and then expressed in terms of the 3-point geodesic Witten diagrams in [65]. On the other hand, the 3-point AdS vertex function with two boundary points reproduces the 3-point geodesic Witten diagram [29]. An explicit expression for the 3-point AdS Feynman diagram with three bulk points was found in [53].

where the  $\kappa$ -coefficients are given by

$$\begin{aligned}\kappa_0 &= \frac{\pi^{\frac{1}{2}}}{2} \frac{\Gamma\left(\frac{h_1+h_2+h_3}{2} - \frac{1}{2}\right)}{\gamma_{h_1 h_2 h_3}} \frac{\Gamma\left(-\frac{h_1+h_2+h_3}{2}\right) \Gamma\left(\frac{h_1-h_2+h_3}{2}\right) \Gamma\left(\frac{h_1+h_2-h_3}{2}\right)}{\Gamma(h_1) \Gamma(h_2) \Gamma(h_3)}, \\ \kappa_n^{(i|jk)} &= \frac{a(h_i; h_j, h_k; n)}{\gamma_{h_j h_k h_{jk|n}}},\end{aligned}\tag{4.2}$$

where the  $a$ -coefficients are given by (2.5) (see our comment below (2.9)), the 3-point structure constants are given by

$$\gamma_{h_1 h_2 h_3} = \left[ \frac{(-2h_1)!(-2h_2)!(-2h_3)!}{\Delta(h_1, h_2, h_3)} \right]^{\frac{1}{2}},\tag{4.3}$$

where  $\Delta(a, b, c) = (-a - b - c + 1)!(c - a - b)!(b - a - c)!(a - b - c)!$  is the modified triangle function. A diagrammatic representation of this expansion is shown in fig. 2.

AdS vertex functions in the Wilson network decomposition (4.1) play the same role as conformal blocks in the conformal block decomposition of the 4-point exchange Witten diagram (2.6), in particular, the groups of single-trace and double-trace terms in the two decompositions have the same conformal dimensions. In other words, the relation (4.1), which was found by brute force calculation of the AdS Feynman diagram, hints at possibility of studying  $n$ -point AdS Feynman diagrams by expanding them into  $n$ -point AdS vertex functions, which, therefore, can be treated as a sort of basis functions in the space of bulk correlation functions. (Similarly, the conformal blocks are basis functions in the space of conformal correlation functions.) At the boundary, they are directly reduced to conformal blocks of single-trace and double-trace intermediate dimensions (one-to-one, without any further transformations or resummations). This provides the conformal block expansion of Witten diagrams. In our  $n = 3$  case the decomposition (4.1) on the conformal boundary reduces to the single-trace term, which is the 3-point conformal correlation function of weights  $h_1, h_2, h_3$  (this is the first term on the right-hand side of (4.1)).<sup>9</sup>

## 4.2 Deriving the Wilson network decomposition

The form of propagator identities (3.2)–(3.4) is very specific, so it is not obvious at all how to find them or other identities of the same type (if any). Consequently, we derive a convenient integral representation of the AdS vertex function that implicitly encodes all three identities and, eventually, the Wilson network decomposition (4.1).

---

<sup>9</sup>This happens only when the triangle inequalities (3.11) are satisfied. In this case the single-trace term is leading near the boundary, whereas the double-trace terms are sub-leading [29] (see also our discussion of the boundary asymptotics in section 3.2). If the triangle inequalities are not satisfied, then the 3-point AdS Feynman diagram on the left-hand side of (4.1) diverges that requires a regularization, see [66] for details.

### 4.2.1 Single-trace contributions

Consider the holographic reconstruction formula for the 3-point AdS vertex function [29]

$$\mathcal{V}_{h_1 h_2 h_3}(\mathbf{x}_1, \mathbf{x}_2, \mathbf{x}_3) = \prod_{k=1}^3 \int_{z_k - i u_k}^{z_k + i u_k} dw_k \mathbb{K}_{h_k}(\mathbf{x}_k, w_k) \langle \mathcal{O}_{h_1}(w_1) \mathcal{O}_{h_2}(w_2) \mathcal{O}_{h_3}(w_3) \rangle, \quad (4.4)$$

where  $\mathbb{K}_{h_k}(\mathbf{x}_k, w_k)$  is the HKLL smearing function (2.3), the 3-point conformal correlation function is given by

$$\langle \mathcal{O}_{h_1}(w_1) \mathcal{O}_{h_2}(w_2) \mathcal{O}_{h_3}(w_3) \rangle = \frac{\gamma_{h_1 h_2 h_3}}{(w_1 - w_2)^{h_1 + h_2 - h_3} (w_2 - w_3)^{h_2 + h_3 - h_1} (w_3 - w_1)^{h_1 + h_3 - h_2}}, \quad (4.5)$$

with the  $\gamma$ -coefficient (4.3), the integral over  $w_k$  is a complex line integral over the line segment connecting points  $z_k - i u_k$  and  $z_k + i u_k$ . The integrals in (4.4) converge only for  $h_i \geq 0$ . The analytic continuation of this relation for  $h_i < 0$  can be obtained by changing integration domains from the line segments to the Pochhammer contours, see [29] for details. Moreover, as we show below, further restriction  $h_i > \frac{1}{2}$  is necessary for our analysis, which we will assume from now on.

Note that the intertwiners in the Wilson network construction which define the left-hand side of (4.4) constrain the weights such that they satisfy the selection rule  $h_2 + h_3 - h_1 \in \mathbb{Z}$ . However, the right-hand side of (4.4) can be used to define the AdS vertex functions for arbitrary non-negative weights  $h_i$ . From now on, we understand AdS vertex functions as the HKLL reconstruction of boundary conformal blocks.

If  $w_i \in \mathbb{R}$ , then the 3-point function (4.5) has known AdS integral representation in terms of the 3-point Witten diagram [67]

$$\langle \mathcal{O}_{h_1}(w_1) \mathcal{O}_{h_2}(w_2) \mathcal{O}_{h_3}(w_3) \rangle = \frac{1}{\kappa_0} \int_{\text{AdS}_2} d^2 \mathbf{x} \sqrt{g(\mathbf{x})} K_{h_1}(\mathbf{x}, w_1) K_{h_2}(\mathbf{x}, w_2) K_{h_3}(\mathbf{x}, w_3), \quad (4.6)$$

where the  $\kappa_0$ -coefficient is given by (4.2), the conformal dimensions  $h_i > \frac{1}{2}$  are subject to the triangle inequalities (3.11). The conditions above, including reality of  $w_i$ , are necessary for the convergence of the AdS integral (4.6).

If  $w_i \in \mathbb{C}$ , then the right-hand side of (4.6) diverges. To see this, rewrite the  $\text{AdS}_2$  integral as a double integral over  $u$  and  $z$  (3.1) and consider poles of the integrand located at  $w_i \pm i u$  on the complex  $z$ -plane,  $i = 1, 2, 3$ , which directly follow from the form of the bulk-to-boundary propagators (2.8). If the integration variable  $u$  takes values  $u = |\text{Im}(w_i)| \neq 0$ , then the integration contour on the  $z$ -plane crosses one of the poles  $w_i + i u$  or  $w_i - i u$  that makes the integral (4.6) divergent.

As the 3-point conformal correlator in the reconstruction formula (4.4) is taken on the complex plane, one should first analytically continue the integral representation (4.6) to the complex plane by deforming the integration contour in the complex  $z$ -plane to avoid crossing

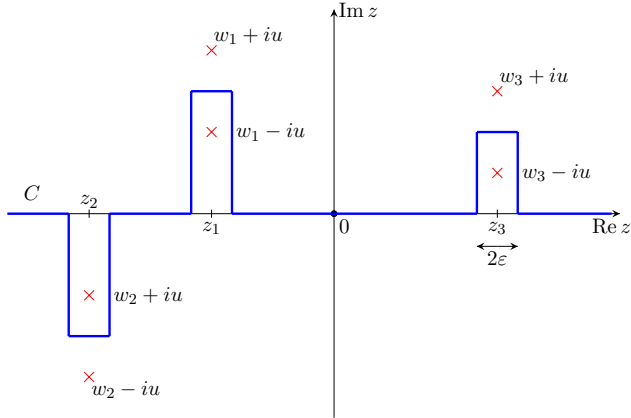


**Figure 5.** The contour  $C$  on the complex  $z$ -plane. The red crosses are poles of the integrand (4.8); the regularization parameter  $\varepsilon \rightarrow 0$ .

the poles. One can show that the analytically continued function reads

$$\begin{aligned} \frac{\kappa_0 \gamma_{h_1 h_2 h_3}}{(w_1 - w_2)^{h_1 + h_2 - h_3} (w_2 - w_3)^{-h_1 + h_2 + h_3} (w_3 - w_1)^{h_1 - h_2 + h_3}} &= \\ &= \int_0^\infty \frac{du}{u^2} \int_C dz K_{h_1}(\mathbf{x}, w_1) K_{h_2}(\mathbf{x}, w_2) K_{h_3}(\mathbf{x}, w_3), \end{aligned} \quad (4.7)$$

where the  $\kappa_0$ -coefficient is given by (4.2) and  $C$  is the contour shown in fig. 5 (see Appendix A for the proof). Substituting (4.7) back into the reconstruction formula (4.4) one obtains

$$\mathcal{V}_{h_1 h_2 h_3}(\mathbf{x}_1, \mathbf{x}_2, \mathbf{x}_3) = \frac{1}{\kappa_0} \prod_{k=1}^3 \int_{z_k - iu_k}^{z_k + iu_k} dw_k \int_0^\infty \frac{du}{u^2} \int_C dz \prod_{m=1}^3 \hat{G}_{h_m}(\mathbf{x}, \mathbf{x}_m, w_m), \quad (4.8)$$

where the modified propagators are defined in (3.5).

Recalling that the single-trace term in the expansion (4.1) is given by the AdS vertex function we see that the integral formula (4.8) can be obtained from the 3-point AdS Feynman diagram by replacing the bulk-to-bulk propagators  $G$  with the modified propagators  $\hat{G}$ , cf. (3.6). However,  $\hat{G}$  has an additional complex variable which should be integrated out by adding one more integral along with changing the integration contours to avoid poles of the new integrand.

#### 4.2.2 Double-trace contributions

To find a similar operation that extracts double-trace contributions, one considers the integral representation (4.8) and divides the integration contour  $C$  into four parts: the first part  $C_0(\varepsilon)$  contains every real line segment of  $C$ , the other three parts are  $\Pi$ -shaped contours bypassing the points  $z_1, z_2, z_3$  on the real axis  $\text{Re } z$ , see fig. 5:

$$C = C_0(\varepsilon) \cup C_1(\varepsilon) \cup C_2(\varepsilon) \cup C_3(\varepsilon), \quad (4.9)$$

where  $\varepsilon$  denotes a half-width of each II-shaped part  $C_{1,2,3}(\varepsilon)$ . All segments are defined so that they are closed intervals near the poles and we will control that the integrals under consideration do not diverge on their endpoints. Roughly speaking, such a splitting of the original contour underlies a decomposition of the AdS Feynman diagram into Wilson networks, where the first non-compact contour corresponds to the single-trace contribution, whereas the other three compact contours correspond to the double-trace contributions. The contour (4.9) splits the AdS vertex function (4.8) into a sum of four integrals:

$$\mathcal{V}_{h_1 h_2 h_3}(\mathbf{x}_1, \mathbf{x}_2, \mathbf{x}_3) = \sum_{i=0}^3 A_{h_1 h_2 h_3}^{(i)}(\mathbf{x}_1, \mathbf{x}_2, \mathbf{x}_3 | \varepsilon) = \sum_{i=0}^3 A_{h_1 h_2 h_3}^{(i)}(\mathbf{x}_1, \mathbf{x}_2, \mathbf{x}_3) + O(\varepsilon), \quad (4.10)$$

where each term  $A_{h_1 h_2 h_3}^{(i)}(\mathbf{x}_1, \mathbf{x}_2, \mathbf{x}_3 | \varepsilon)$  is given by the integral (4.8) restricted on the corresponding part of the whole contour  $C$ , and

$$A_{h_1 h_2 h_3}^{(i)}(\mathbf{x}_1, \mathbf{x}_2, \mathbf{x}_3) \equiv \lim_{\varepsilon \rightarrow 0} A_{h_1 h_2 h_3}^{(i)}(\mathbf{x}_1, \mathbf{x}_2, \mathbf{x}_3 | \varepsilon). \quad (4.11)$$

At this stage, we assume that the limits in (4.11) do exist that we explicitly verify later in this section. By construction, the left-hand side of (4.10) is independent of the regularization parameter  $\varepsilon$ . It follows that  $O(\varepsilon)$  terms in (4.10) add up to zero and, therefore, can be neglected.

Let us consider the first term in (4.10):

$$\begin{aligned} A_{h_1 h_2 h_3}^{(0)}(\mathbf{x}_1, \mathbf{x}_2, \mathbf{x}_3 | \varepsilon) &= \frac{1}{\kappa_0} \prod_{k=1}^3 \int_{z_k - iu_k}^{z_k + iu_k} dw_k \int_0^\infty \frac{du}{u^2} \int_{C_0(\varepsilon)} dz \prod_{m=1}^3 \widehat{G}_{h_m}(\mathbf{x}, \mathbf{x}_m, w_m) \\ &= \frac{1}{\kappa_0} \int_0^\infty \frac{du}{u^2} \int_{C_0(\varepsilon)} dz \prod_{k=1}^3 \int_{z_k - iu_k}^{z_k + iu_k} dw_k \widehat{G}_{h_k}(\mathbf{x}, \mathbf{x}_k, w_k) \\ &= \frac{1}{\kappa_0} \int_0^\infty \frac{du}{u^2} \int_{C_0(\varepsilon)} dz G_{h_1}(\mathbf{x}, \mathbf{x}_1) G_{h_2}(\mathbf{x}, \mathbf{x}_2) G_{h_3}(\mathbf{x}, \mathbf{x}_3). \end{aligned} \quad (4.12)$$

Here, the second line is obtained by interchanging the integrals over  $w_k$  and  $u, z$ . Note that this was not possible in the integral (4.8) due to the fact that  $C$  depends on  $w_k$ , whereas  $C_0(\varepsilon)$  does not. The last line results from the following lemma.

**Lemma 1 (the conversion identity)** *The  $AdS_2$  bulk-to-bulk scalar propagator has the following integral representation:*

$$G_h(\mathbf{x}, \mathbf{x}') = \int_{z' - iu'}^{z' + iu'} dw \widehat{G}_h(\mathbf{x}, \mathbf{x}', w), \quad \text{Re}(z) \neq \text{Re}(z') \text{ or } u > u' - |\text{Im}(z - z')|, \quad h > 0, \quad (4.13)$$

where  $\mathbf{x} = (u, z)$ ,  $\mathbf{x}' = (u', z')$  and

$$G_h(\mathbf{x}, \mathbf{x}') = \left( \frac{uu'}{u^2 + u'^2 + (z - z')^2} \right)^h {}_2F_1 \left[ \frac{h}{2}, \frac{h}{2} + \frac{1}{2}; h + \frac{1}{2} \middle| \left( \frac{2uu'}{u^2 + u'^2 + (z - z')^2} \right)^2 \right], \quad (4.14)$$

$$\widehat{G}_h(\mathbf{x}, \mathbf{x}', w) = \frac{-2i}{4^h} \frac{\Gamma(2h)}{\Gamma(h)\Gamma(h)} \left( \frac{u'}{u'^2 + (z' - w)^2} \right)^{1-h} \left( \frac{u}{u^2 + (z - w)^2} \right)^h ; \quad (4.15)$$

$u, u' \in \mathbb{R}$  and  $w, z, z' \in \mathbb{C}$ .

The proof is given in Appendix B.1. By applying Lemma 1 to other three terms in (4.10) one finds that ( $i \neq j \neq k \neq i$ )

$$\begin{aligned} A_{h_1 h_2 h_3}^{(i)}(\mathbf{x}_1, \mathbf{x}_2, \mathbf{x}_3 | \varepsilon) &= \\ &= \frac{1}{\kappa_0} \int_{z_i - iu_i}^{z_i + iu_i} dw_i \int_0^\infty \frac{du}{u^2} \int_{C_i(\varepsilon)} dz \widehat{G}_{h_i}(\mathbf{x}, \mathbf{x}_i, w_i) G_{h_j}(\mathbf{x}, \mathbf{x}_j) G_{h_k}(\mathbf{x}, \mathbf{x}_k), \end{aligned} \quad (4.16)$$

where the contour  $C_i(\varepsilon)$  is shown in fig. 6. Now, taking the limit  $\varepsilon \rightarrow 0$  in the first term yields the 3-point AdS Feynman diagram

$$A_{h_1 h_2 h_3}^{(0)}(\mathbf{x}_1, \mathbf{x}_2, \mathbf{x}_3) = \frac{1}{\kappa_0} \int_{\text{AdS}_2} d^2 \mathbf{x} \sqrt{g(\mathbf{x})} G_{h_1}(\mathbf{x}, \mathbf{x}_1) G_{h_2}(\mathbf{x}, \mathbf{x}_2) G_{h_3}(\mathbf{x}, \mathbf{x}_3). \quad (4.17)$$

Indeed, in this case  $\lim_{\varepsilon \rightarrow 0} C_0(\varepsilon) = \mathbb{R}$ , and the right-hand side in (4.12) exactly reproduces the 3-point AdS Feynman diagram. The limit  $\varepsilon \rightarrow 0$  exists as the integrand has no poles in the domain  $\mathbf{x} \in \mathbb{R}_{\geq 0} \times \mathbb{R}$ .

Thus, by means of (4.10) the AdS vertex function can be represented as

$$\begin{aligned} \mathcal{V}_{h_1 h_2 h_3}(\mathbf{x}_1, \mathbf{x}_2, \mathbf{x}_3) &= \frac{1}{\kappa_0} \int_{\text{AdS}_2} d^2 \mathbf{x} \sqrt{g(\mathbf{x})} G_{h_1}(\mathbf{x}, \mathbf{x}_1) G_{h_2}(\mathbf{x}, \mathbf{x}_2) G_{h_3}(\mathbf{x}, \mathbf{x}_3) + O(\varepsilon) \\ &+ A_{h_1 h_2 h_3}^{(1)}(\mathbf{x}_1, \mathbf{x}_2, \mathbf{x}_3 | \varepsilon) + A_{h_1 h_2 h_3}^{(2)}(\mathbf{x}_1, \mathbf{x}_2, \mathbf{x}_3 | \varepsilon) + A_{h_1 h_2 h_3}^{(3)}(\mathbf{x}_1, \mathbf{x}_2, \mathbf{x}_3 | \varepsilon). \end{aligned} \quad (4.18)$$

This formula reminds the decomposition (4.1): they both relate the 3-point AdS Feynman diagram and the 3-point AdS vertex function and involve three additional (groups of) terms. Although the additional terms from these relations are different in form (integrals vs infinite sums), they are similar in their properties. E.g. these terms share the same property of transforming into each other under the cyclic permutation of conformal weights and coordinates. Also, near-boundary ( $u \rightarrow 0$ ) expansions of additional terms from (4.18) and (4.1) have pairwise the same powers of the  $u$ -coordinate. Below we formulate three Lemmas which are used to prove that  $A_{h_1 h_2 h_3}^{(i)}(\mathbf{x}_1, \mathbf{x}_2, \mathbf{x}_3 | \varepsilon)$ ,  $i = 1, 2, 3$ , from (4.18) is proportional to the  $(i + 1)$ -th term on the right-hand side of (4.1) (assuming the obvious line-by-line enumeration).

**Lemma 2** *Let  $C_i(\varepsilon)$  be the contour shown in fig. 6 and  $f(\mathbf{x})$  be a holomorphic function on a domain  $U \times V \subset \mathbb{C}^2$  of complex argument  $\mathbf{x} = (u, z)$ , such that  $U \subset \mathbb{R}$  and  $V \subset C_i(\varepsilon)$  for any  $\varepsilon \rightarrow 0$ . Let  $f(\mathbf{x})$  satisfy  $u^{-h_i} f(\mathbf{x}) \rightarrow 0$  at  $u \rightarrow 0$  for some  $h_i > 0$ . Then, the following identity holds*

$$\lim_{\varepsilon \rightarrow 0} \int_{z_i - iu_i}^{z_i + iu_i} dw_i \int_0^\infty \frac{du}{u^2} \int_{C_i(\varepsilon)} dz \widehat{G}_{h_i}(\mathbf{x}, \mathbf{x}_i, w_i) f(\mathbf{x}) = \pi \int_0^{u_i} \frac{du}{u^2} \int_{z_i - i(u_i - u)}^{z_i + i(u_i - u)} dz \widetilde{G}_{h_i}(\mathbf{x}, \mathbf{x}_i) f(\mathbf{x}), \quad (4.19)$$

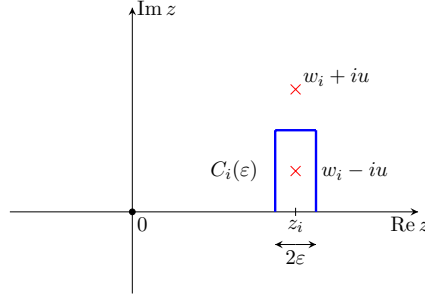


**Figure 6.** The contour  $C_i(\varepsilon)$  on the complex  $z$ -plane,  $i = 1, 2, 3$ . The red crosses are poles in (4.16).

where  $\mathbf{x}_i = (u_i, z_i)$ , and

$$\tilde{G}_{h_i}(\mathbf{x}, \mathbf{x}_i) = \frac{-2i}{4^{h_i}} \frac{\Gamma(2h_i)}{\Gamma(h_i)\Gamma(h_i)} \left( \frac{\Gamma(1-2h_i)}{\Gamma(1-h_i)^2} G_{h_i}(\mathbf{x}, \mathbf{x}_i) + \frac{\Gamma(2h_i-1)}{\Gamma(h_i)^2} G_{1-h_i}(\mathbf{x}, \mathbf{x}_i) \right); \quad (4.20)$$

$G_{h_i}(\mathbf{x}, \mathbf{x}_i)$  and  $\tilde{G}_{h_i}(\mathbf{x}, \mathbf{x}_i, w_i)$  are given by (4.14) and (4.15).

The proof is given in Appendix **B.2**.

**Lemma 3 (the splitting identity)** *The following integral identity holds*

$$\begin{aligned} & \int_0^{u_3} \frac{du}{u^2} \int_{z_3-i(u-u_3)}^{z_3+i(u-u_3)} dz G_{h_1}(\mathbf{x}, \mathbf{x}_1) G_{h_2}(\mathbf{x}, \mathbf{x}_2) \tilde{G}_{h_3}(\mathbf{x}, \mathbf{x}_3) = \frac{1}{8i\pi^3} \frac{(-)^{h_1+h_2}}{\sin(2\pi(h_1+h_2))} \\ & \times \sum_{n=0}^{\infty} \frac{a(h_3; h_1, h_2; n)}{\alpha'_{h_1 h_2, n}} \int_{z_3-iu_3}^{z_3+iu_3} dw \oint_0 \frac{du}{u^2} \oint_{P[w-iu, w+iu]} dz G_{h_1}(\mathbf{x}, \mathbf{x}_1) G_{h_2}(\mathbf{x}, \mathbf{x}_2) \tilde{G}_{h_{12|n}}(\mathbf{x}, \mathbf{x}_3, w), \end{aligned} \quad (4.21)$$

where the  $a$ -coefficients are given by (2.5), the coefficient  $\alpha'_{h_1 h_2, n}$  is given by

$$\alpha'_{h_1 h_2, n} = \frac{(-)^n}{2\pi^{\frac{1}{2}} i} \frac{\Gamma(h_1 + h_2 + n - \frac{1}{2})\Gamma(h_1 + n)\Gamma(h_2 + n)}{n! \Gamma(h_1 + h_2 + 2n)\Gamma(h_1)\Gamma(h_2)}; \quad (4.22)$$

$P[w - iu, w + iu]$  is the Pochhammer contour around points  $w - iu$  and  $w + iu$ , see fig. 4.

**Corollary 1** *The splitting identity (4.21) can be cast into the following form:*

$$\int_0^{u_3} \frac{du}{u^2} \int_{z_3-i(u-u_3)}^{z_3+i(u-u_3)} dz G_{h_1}(\mathbf{x}, \mathbf{x}_1) G_{h_2}(\mathbf{x}, \mathbf{x}_2) \tilde{G}_{h_3}(\mathbf{x}, \mathbf{x}_3) = \frac{1}{\pi} \sum_{n=0}^{\infty} \kappa_n^{(3|12)} \mathcal{V}_{h_1 h_2 h_{12|n}}(\mathbf{x}_1, \mathbf{x}_2, \mathbf{x}_3), \quad (4.23)$$

where  $\mathcal{V}_{h_1 h_2 h_{12|n}}(\mathbf{x}_1, \mathbf{x}_2, \mathbf{x}_3)$  is the 3-point  $AdS$  vertex function and the coefficient  $\kappa_n^{(3|12)}$  is given by (4.2).

The proofs are given in Appendix B.3. Then, it is straightforward to see that applying Lemma 2 and Lemma 3 as well as Corollary 1 to (4.16) one obtains

$$\begin{aligned} A_{h_1 h_2 h_3}^{(i)}(\mathbf{x}_1, \mathbf{x}_2, \mathbf{x}_3) &= \frac{\pi}{\kappa_0} \int_0^{u_i} \frac{du}{u^2} \int_{z_i-i(u_i-u)}^{z_i+i(u_i-u)} dz \tilde{G}_{h_i}(\mathbf{x}, \mathbf{x}_i) G_{h_j}(\mathbf{x}, \mathbf{x}_j) G_{h_k}(\mathbf{x}, \mathbf{x}_k) \\ &= -\frac{1}{\kappa_0} \sum_{n=0}^{\infty} \kappa_n^{(i|jk)} \mathcal{V}_{h_j h_k h_{jk|n}}(\mathbf{x}_j, \mathbf{x}_k, \mathbf{x}_i), \quad i \neq j \neq k \neq i. \end{aligned} \quad (4.24)$$

Thus, along with (4.17) these relations prove the decomposition of the 3-point AdS Feynman diagram (4.1) into 3-point AdS vertex functions without calculating them explicitly. Note that by acting with the KG operator  $\square_{\mathbf{x}_i} - h_i(h_i - 1)$  to the first and second line of (4.24) one obtains the following identity:

$$\begin{aligned} &\frac{2\sqrt{\pi} \Gamma(h_i + \frac{1}{2})}{\Gamma(h_i)} G_{h_j}(\mathbf{x}_j, \mathbf{x}_i) G_{h_k}(\mathbf{x}_k, \mathbf{x}_i) \\ &= \sum_{n=0}^{\infty} (h_{jk|n}(h_{jk|n} - 1) - h_i(h_i - 1)) \kappa_n^{(i|jk)} \mathcal{V}_{h_j h_k h_{jk|n}}(\mathbf{x}_j, \mathbf{x}_k, \mathbf{x}_i), \quad i \neq j \neq k \neq i, \end{aligned} \quad (4.25)$$

where we used that AdS vertex functions solve the homogeneous KG equations [27].<sup>10</sup>

#### 4.2.3 Superposition identity

The relation (4.24) shows that the change  $G_{h_i} \rightarrow \tilde{G}_{h_i}$ , supplemented by the change of the integration contour in the  $z$ -plane, allows us to single out the double-trace terms. In other words, the relations (4.8) and (4.24) present a method of extracting single-trace and double-trace terms from the AdS Feynman diagram by replacing bulk-to-bulk propagators with modified propagators. In what follows, we show that this can be formalized by introducing an identity which expands a bulk-to-bulk propagator into modified propagators.

**Lemma 4 (the superposition identity)** *Let  $f(\mathbf{x})$  be a test function satisfying the conditions of Lemma 2. Let  $C_i(\varepsilon)$  be the contour shown in fig. 6, and  $C(\varepsilon) + C_i(\varepsilon)$  be a continuous curve. Here,  $C(\varepsilon)$  is any contour on the complex  $z$ -plane that avoids the poles of  $f(\mathbf{x})$  and satisfies  $\text{Re}(z) \neq z_i, \forall z \in C(\varepsilon)$ . The following identity then holds:*

$$\begin{aligned} \lim_{\varepsilon \rightarrow 0} \int_0^{\infty} \frac{du}{u^2} \int_{C(\varepsilon)} dz G_{h_i}(\mathbf{x}, \mathbf{x}_i) f(\mathbf{x}) &= \pi \int_0^{u_i} \frac{du}{u^2} \int_{z_i-i(u-u_i)}^{z_i+i(u-u_i)} dz \tilde{G}_{h_i}(\mathbf{x}, \mathbf{x}_i) f(\mathbf{x}) \\ &+ \lim_{\varepsilon \rightarrow 0} \int_{z_i-iu_i}^{z_i+iu_i} dw_i \int_0^{\infty} \frac{du}{u^2} \int_{C(\varepsilon)+C_i(\varepsilon)} dz \hat{G}_{h_i}(\mathbf{x}, \mathbf{x}_i, w_i) f(\mathbf{x}), \end{aligned} \quad (4.26)$$

where  $G_{h_i}(\mathbf{x}, \mathbf{x}_i)$ ,  $\hat{G}_{h_i}(\mathbf{x}, \mathbf{x}_i, w_i)$ ,  $\tilde{G}_{h_i}(\mathbf{x}, \mathbf{x}_i)$  are given by (4.14), (4.15), (4.20), respectively.

---

<sup>10</sup>This identity can also be proved directly by using explicit expressions for the 3-point AdS vertex functions found in [29].

The proof is given in Appendix B.4. Note that the integration domains in (4.26) and (3.3) are different. For the sake of simplicity, the latter identity is given for the Poincare patch,  $\mathbf{x} \in \mathbb{R}_{\geq 0} \times \mathbb{R}$ , see the right-hand side of (3.3). Indeed, the relation (3.3) is the special case of the relation (4.26) obtained by changing  $\mathbf{x}_i \rightarrow \mathbf{x}'$ ,  $w_i \rightarrow w$ ,  $h_i \rightarrow h$  and  $C(\varepsilon) + C_i(\varepsilon) \rightarrow C$ , where  $C(\varepsilon) = \mathbb{R} \setminus U_\varepsilon(z')$ , see fig. 4.

Furthermore, the general form of the superposition identity (4.26) allows one to expand a product of  $n$  bulk-to-bulk propagators integrated over a bulk point using the following lemma, which is a direct generalization of Lemma 4.

**Lemma 5 (the multipoint superposition identity)** *Let  $f(\mathbf{x})$  be a test function satisfying the conditions of Lemma 2. Applying Lemma 4 to the product of  $n$  bulk-to-bulk propagators  $n$  times yields*

$$\begin{aligned} & \int_0^\infty \frac{du}{u^2} \int_{\mathbb{R}} dz \prod_{i=1}^n G_{h_i}(\mathbf{x}, \mathbf{x}_i) f(\mathbf{x}) \\ &= \pi \sum_{k=1}^n \int_0^{u_k} \frac{du}{u^2} \int_{z_k - i(u-u_k)}^{z_k + i(u-u_k)} dz \left( \prod_{\substack{i=1 \\ i \neq k}}^n \int_{z_i - iu_i}^{z_i + iu_i} dw_i \widehat{G}_{h_i}(\mathbf{x}, \mathbf{x}_i) \right) \widetilde{G}_{h_k}(\mathbf{x}, \mathbf{x}_k) f(\mathbf{x}) \quad (4.27) \\ &+ \lim_{\substack{\varepsilon_i \rightarrow 0 \\ i=1, \dots, n}} \left( \prod_{i=1}^n \int_{z_i - iu_i}^{z_i + iu_i} dw_i \right) \int_0^\infty \frac{du}{u^2} \int_{C(\varepsilon_1, \dots, \varepsilon_n)} dz \left( \prod_{k=1}^n \widehat{G}_{h_k}(\mathbf{x}, \mathbf{x}_k, w_k) \right) f(\mathbf{x}), \end{aligned}$$

where the contour  $C(\varepsilon_1, \dots, \varepsilon_n)$  is given by

$$C(\varepsilon_1, \dots, \varepsilon_n) = \mathbb{R} \setminus \bigcup_{i=1}^n U_{\varepsilon_i}(z_i) + \sum_{i=1}^n C_i(\varepsilon_i), \quad (4.28)$$

where  $U_{\varepsilon_i}(z_i)$  is the  $\varepsilon_i$ -neighbourhood of the point  $z_i$  (see fig. 7).

The proof is given in Appendix B.5. The only significant change here compared to Lemma 4 is the form of the  $n$ -point contour. Note that choosing  $f(\mathbf{x}) = 1$  immediately gives the superposition identity for the  $n$ -point contact AdS Feynman diagram, the schematic form of which is given in (3.12).

The (multipoint) superposition identity allows one to decompose AdS Feynman diagrams into diagrams with modified propagators. In the case of the 3-point AdS Feynman diagram this decomposition reads

$$\begin{aligned} & \int_{\text{AdS}_2} d^2 \mathbf{x} \sqrt{g(\mathbf{x})} G_{h_1}(\mathbf{x}, \mathbf{x}_1) G_{h_2}(\mathbf{x}, \mathbf{x}_2) G_{h_3}(\mathbf{x}, \mathbf{x}_3) \\ &= \kappa_0 \prod_{k=1}^3 \int_{z_k - iu_k}^{z_k + iu_k} dw_k \int_0^\infty \frac{du}{u^2} \int_C dz \prod_{i=1}^3 \widehat{G}_{h_i}(\mathbf{x}, \mathbf{x}_i, w_i) \\ &+ \pi \left( \int_0^{u_1} \frac{du}{u^2} \int_{z_1 - i(u-u_1)}^{z_1 + i(u-u_1)} dz \widetilde{G}_{h_1}(\mathbf{x}, \mathbf{x}_1) \prod_{i=2}^3 \int_{z_i - iu_i}^{z_i + iu_i} dw_i \widehat{G}_{h_i}(\mathbf{x}, \mathbf{x}_i) + (1 \leftrightarrow 2) + (1 \leftrightarrow 3) \right), \quad (4.29) \end{aligned}$$

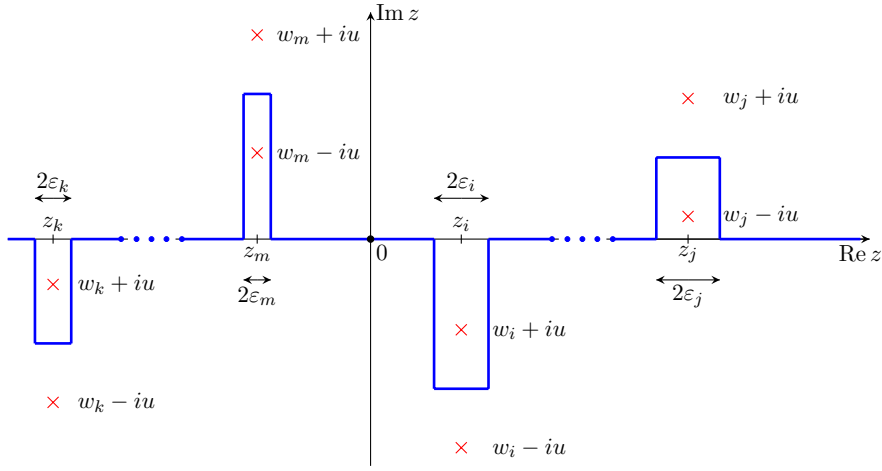


**Figure 7.** The contour  $C(\varepsilon_1, \dots, \varepsilon_n)$  on the complex  $z$ -plane.

which directly follows from (4.27). This is the detailed form of the relation (3.7). The properties of each term on the right-hand side of the relation were discussed in section 3. The graphical representation of (4.29) in terms of modified bulk-to-bulk propagators is shown in fig. 8.

Note that the (multipoint) superposition identity does not produce infinite sums of double-trace terms, they are further generated by applying the splitting identity (4.21). Following the algorithm for decomposing the 3-point AdS Feynman diagram discussed in section 3, one obtains the known decomposition of the 3-point AdS Feynman diagram into the AdS vertex functions (4.1):

$$\begin{aligned}
\text{right-hand side of (4.29)} &= \kappa_0 \prod_{k=1}^3 \int_{z_k-iu_k}^{z_k+iu_k} dw_k \int_0^\infty \frac{du}{u^2} \int_C dz \prod_{i=1}^3 \widehat{G}_{h_i}(\mathbf{x}, \mathbf{x}_i, w_i) \\
&+ \frac{1}{8\pi^2} \left( \frac{(-)^{h_2+h_3}}{\sin(2\pi(h_2+h_3))} \sum_{n=0}^\infty \frac{a(h_1; h_2, h_3; n)}{\alpha'_{h_2 h_3, n}} \int_{z_k-iu_k}^{z_k+iu_k} dw_k \oint_0^\infty \frac{du}{u^2} \oint_{P[w_1-iu, w_1+iu]} dz \right. \\
&\times \left. \widehat{G}_{h_{23|n}}(\mathbf{x}, \mathbf{x}_1, w_1) \widehat{G}_{h_2}(\mathbf{x}, \mathbf{x}_2, w_2) \widehat{G}_{h_3}(\mathbf{x}, \mathbf{x}_3, w_3) + (1 \leftrightarrow 2) + (1 \leftrightarrow 3) \right) \\
&= \kappa_0 \mathcal{V}_{h_1 h_2 h_3}(\mathbf{x}_1, \mathbf{x}_2, \mathbf{x}_3) + \left( \sum_{n=0}^\infty \kappa_n^{(1|23)} \mathcal{V}_{h_{23|n} h_2 h_3}(\mathbf{x}_1, \mathbf{x}_2, \mathbf{x}_3) + (1 \leftrightarrow 2) + (1 \leftrightarrow 3) \right), \tag{4.30}
\end{aligned}$$

where the contours  $C$  and  $P$  are shown in fig. 5 and fig. 4 (b). The first equality is obtained by applying the splitting identity (4.21) to the terms in the third line of (4.29). The last equality is obtained by observing that the first line in (4.30) is just the integral representation of the AdS vertex function (4.8); similarly, the second and third lines are given by (4.23).

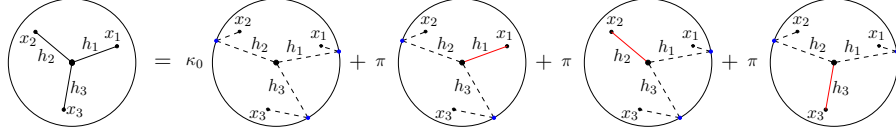


**Figure 8.** The decomposition of the 3-point AdS Feynman diagram into diagrams with modified propagators (4.29). The black lines are the bulk-to-bulk propagators  $G_h(\mathbf{x}, \mathbf{x}')$ , the red lines are the modified propagators  $\tilde{G}_h(\mathbf{x}, \mathbf{x}')$ , the dashed broken lines are the modified propagators  $\hat{G}_h(\mathbf{x}, \mathbf{x}', w)$ . The integrations over  $w$  are shown by cusps located on the boundary.

## 5 Conclusion and outlooks

In this work, we have shown that AdS Feynman diagrams can be decomposed into Wilson network matrix elements, which serve as a kind of basis functions. We have considered the simplest case of the scalar 3-point AdS Feynman diagram in Euclidean  $\text{AdS}_2$  space, demonstrating that such a decomposition involves both a single-trace term and infinite sums of double-trace terms (terminology derived from the standard running conformal dimensions), thereby mimicking the conformal block decomposition of Witten diagrams. There are two key ingredients in this construction: first, we utilize AdS integral propagator identities that transform the AdS Feynman diagram into an infinite sum of terms; second, each term can be represented as a particular Wilson network matrix element.

Our results can be extended in several directions. First, one may generalize the proposed method to the  $n$ -point case with intermediate channels. The first interesting case here is the 4-point exchange AdS Feynman diagram. It is now evident that similar decompositions into Wilson networks can be achieved by applying the superposition identity to the internal lines and finding the  $n$ -point splitting identity that would relate the  $n$ -point modified AdS Feynman diagrams and  $n$ -point AdS vertex functions. It is also interesting to see how the Wilson network decomposition can be extended to arbitrary spin fields in  $d$  dimensions. Specifically, the  $d$ -dimensional Wilson line networks and their near-boundary asymptotics were considered in [16] (for more on higher-dimensional spin-networks in the present context see [68] and e.g. [69]). Of course, the search for various AdS propagator identities in both Euclidean and Lorentzian  $\text{AdS}_{d+1}$  space is interesting in itself.

**Acknowledgements.** We are grateful to Semyon Mandrygin for useful discussions. Our work was partially supported by the Foundation for the Advancement of Theoretical Physics and Mathematics “BASIS”.

## A Analytic continuation of the 3-point Witten diagram

Let us consider the 3-point Witten diagram [67]

$$\frac{1}{\kappa_0} \int_0^\infty \frac{du}{u^2} \int_{\mathbb{R}} dz K_{h_1}(\mathbf{x}, w_1) K_{h_2}(\mathbf{x}, w_2) K_{h_3}(\mathbf{x}, w_3) = \langle \mathcal{O}_{h_1}(w_1) \mathcal{O}_{h_2}(w_2) \mathcal{O}_{h_3}(w_3) \rangle, \quad (\text{A.1})$$

where  $\mathbf{x} = (u, z)$ ,  $w_i \in \mathbb{R}$ ,  $w_i \neq w_j$ ,  $\kappa_0$  is defined in (4.2),  $h_i > \frac{1}{2}$  satisfy the triangle inequalities (3.11). The integral converges only when  $w_i$  are real, whereas the HKLL procedure requires integrating (A.1) over complex  $w_i$  with a particular kernel (see section 4.2.1). To this end, one first considers the following integral

$$\begin{aligned} I_{\mathbb{R}}(w_1, w_2, w_3; \varepsilon) &\equiv \int_{\varepsilon}^{\infty} \frac{du}{u^2} \int_{\mathbb{R}} dz K_{h_1}(\mathbf{x}, w_1) K_{h_2}(\mathbf{x}, w_2) K_{h_3}(\mathbf{x}, w_3) \\ &= \int_{\varepsilon}^{\infty} \frac{du}{u^2} u^{h_1+h_2+h_3} \int_{\mathbb{R}} dz \prod_{i=1}^3 (u^2 + (w_i - z)^2)^{-h_i}, \end{aligned} \quad (\text{A.2})$$

where  $\varepsilon > 0$ ,  $w_i \in \mathbb{C}$ ,  $\text{Re}(w_i) \neq \text{Re}(w_j)$  for any  $i \neq j$ ,  $h_i$  are subject to the same restrictions as in (A.1), and we substituted the bulk-to-boundary propagator (2.8). As the original integral (A.1) is obtained from  $I_{\mathbb{R}}(w_1, w_2, w_3; \varepsilon)$  by taking the limit  $\varepsilon \rightarrow 0$ , the analytic continuation of (A.2) also provides the analytic continuation of the original integral by taking the limit  $\varepsilon \rightarrow 0$ .

The integral  $I_{\mathbb{R}}(w_1, w_2, w_3; \varepsilon)$  converges only when  $|\text{Im}(w_i)| < \varepsilon$ . This follows from that the integrals in (A.2) converge iff singularities of the integrand do not lie in the integration domain of  $I_{\mathbb{R}}$ . If  $|\text{Im}(w_i)| \geq \varepsilon$  for some  $i$ , then a singularity of the integrand located at  $(u, z) = (|\text{Im}(w_i)|, \text{Re}(w_i))$  lies in the integration domain  $(u, z) \in [\varepsilon, \infty) \times \mathbb{R}$ , thereby producing the divergence.

In order to analytically continue  $I_{\mathbb{R}}(w_1, w_2, w_3; \varepsilon)$  to the domain  $|\text{Im}(w_i)| \geq \varepsilon$  one considers the following integral

$$I_{C(y_1, y_2, y_3)}(w_1, w_2, w_3; \varepsilon) \equiv \int_{\varepsilon}^{\infty} \frac{du}{u^2} \int_{C(y_1, y_2, y_3)} dz K_{h_1}(\mathbf{x}, w_1) K_{h_2}(\mathbf{x}, w_2) K_{h_3}(\mathbf{x}, w_3), \quad (\text{A.3})$$

where  $y_i \in \mathbb{R}$  and the contour  $C(y_1, y_2, y_3)$  is shown in fig. 9. Then, the singularities of the integrand in (A.3) do not lie in the integration domain only when  $|\text{Im}(w_i) - y_i| < \varepsilon$ . Thus, (A.3) provides the analytic continuation of  $I_{\mathbb{R}}$  in  $w_i \in \mathbb{C}$ , such that  $|\text{Im}(w_i) - y_i| < \varepsilon$ , i.e. by choosing different parameters  $y_i$  in the integration contour one obtains the analytic continuation for different domains of  $w_i$ . There are two distinct cases in the proof of this statement: (1)  $|y_i| < 2\varepsilon$ ; (2)  $|y_i| \geq 2\varepsilon$ . To simplify the proof we focus on the analytic continuation in one variable  $w_i$  only, e.g.  $i = 1$  and  $y_2 = y_3 = 0$ ; the proof for other variables is similar.

In the first case  $|y_1| < 2\varepsilon$ , without loss of generality, we fix  $y_1 > 0$ . The case  $y_1 < 0$  can be proved similarly, and the case  $y_1 = 0$  is trivial since  $C(0, 0, 0) = \mathbb{R}$  and  $I_{C(0, 0, 0)} = I_{\mathbb{R}}$ . To see that (A.3) provides analytic continuation of (A.2), one shows that the integrals coincide in the domain where they both converge. The integral  $I_C$  converges when  $y_1 - \varepsilon < \text{Im}(w_i) < y_1 + \varepsilon$ , whereas the integral  $I_{\mathbb{R}}$  converges when  $-\varepsilon < \text{Im}(w_i) < \varepsilon$ . Due to the restriction  $0 < y_1 < 2\varepsilon$  these domains of convergence have non-empty overlap  $y_1 - \varepsilon < \text{Im}(w_i) < \varepsilon$ .  $I_{\mathbb{R}}$  and  $I_C$  coincide in this domain, as there exists a continuous deformation that transforms the contour  $C(y_1, y_2, y_3)$  to the line contour without crossing singularities or branch cuts of the integrand, see fig. 9 (b). This proves the analytic continuation for  $|y_1| < 2\varepsilon$ .

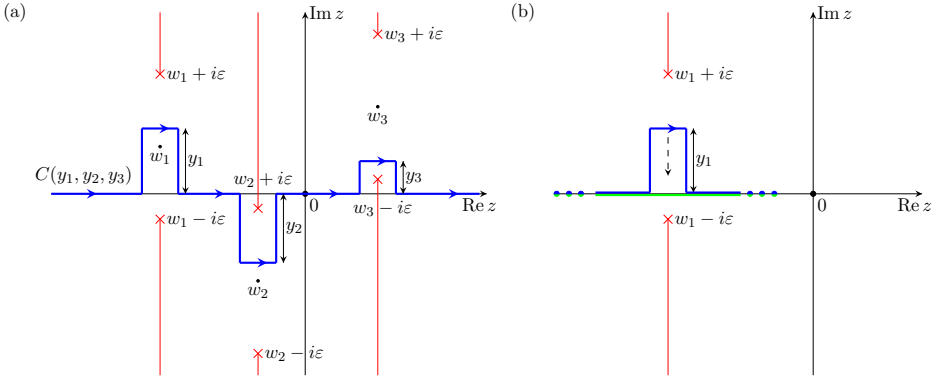


**Figure 9.** (a) The contour  $C(y_1, y_2, y_3)$  on the complex  $z$ -plane  $\mathbb{C}$ . The red crosses and lines show possible singularities of the integrand in (A.2), i.e. if  $z$  is taken on the red line, then  $\exists u \in [\varepsilon, \infty)$  such that the integrand is singular in  $(u, z)$ . Note that for such a choice of  $w_i$  and  $\varepsilon$  the integral  $I_{\mathbb{R}}$  diverges because possible singularities cross the integration contour which is the real line  $z \in \mathbb{R}$  in this case. Changing the line contour in  $I_{\mathbb{R}}$  to the contour  $C(y_1, y_2, y_3)$  allows one to avoid crossing singularities and, therefore, analytically continue  $I_{\mathbb{R}}$  to any complex  $w_i$ . (b) The blue line corresponds to the contour  $C(y_1, y_2, y_3)$ , the green line corresponds to the line contour. The dashed arrow describes a deformation of  $C(y_1, y_2, y_3)$  to the line contour. Note that the restriction  $y_1 - \varepsilon < \text{Im}(w_i) < \varepsilon$  ensures that the possible singularities do not lie on any contour.

In the second case  $y_1 \geq 2\varepsilon$ , where we also fixed  $y_1 > 0$ , the overlap of domains of convergence of  $I_C$  and  $I_{\mathbb{R}}$  is empty. To show this, one introduces a chain of analytically continued integrals starting from the original integral  $I_{\mathbb{R}}$  and ending with the integral  $I_{C(y_1, y_2, y_3)}$ , where a non-empty overlap of domains of convergence exists only for nearest neighbours. This can be done by introducing  $n$  auxiliary variables  $\alpha_k = ky_1/n$  such that  $\alpha_k - \alpha_{k-1} < 2\varepsilon$  and defining  $n$  integrals  $I_{C(\alpha_k, y_2, y_3)}$ . To show that  $I_{C(\alpha_k, y_2, y_3)}$  analytically continues  $I_{C(\alpha_{k-1}, y_2, y_3)}$  one applies the same arguments as in the case  $|y_1| < 2\varepsilon$ , because the restriction  $\alpha_k - \alpha_{k-1} < 2\varepsilon$  ensures that the domains of convergence of these integrals intersect. The contour  $C(\alpha_k, y_2, y_3)$  in this domain can be continuously deformed to the contour  $C(\alpha_{k-1}, y_2, y_3)$ , this can be done as in fig. 9 (b). Thus,  $I_{C(\alpha_k, y_2, y_3)} = I_{C(\alpha_{k-1}, y_2, y_3)}$  in the domain where both integrals converge. This proves the analytic continuation for  $|y_1| \geq 2\varepsilon$ .

We have shown that the analytic continuation of (A.2) to any  $w_1 \in \mathbb{C}$  can be achieved by changing the integration contour. Repeating the proof for other variables  $w_2$  and  $w_3$ , one obtains the following analytic continuation of the integral (A.2):

$$\int_{\varepsilon}^{\infty} \frac{du}{u^2} \int_C dz K_{h_1}(\mathbf{x}, w_1) K_{h_2}(\mathbf{x}, w_2) K_{h_3}(\mathbf{x}, w_3), \quad (\text{A.4})$$

where  $w_i \neq w_j$  for any  $i \neq j$  and the contour  $C \equiv C(\text{Im}(w_1), \text{Im}(w_2), \text{Im}(w_3))$  is shown in fig. 5. Note that the variables  $y_i$  in  $C(y_1, y_2, y_3)$  are chosen to be equal to  $\text{Im}(w_i)$ . In this way, one ensures that the domain of convergence of (A.4) does not depend on  $\varepsilon$ : it is given by

$|\operatorname{Im}(w_i) - y_i| < \varepsilon$ , and, therefore, in the case  $y_i = \operatorname{Im}(w_i)$ , the restriction is satisfied for any  $\varepsilon > 0$  and  $w_i \in \mathbb{C}$ . By taking the limit  $\varepsilon \rightarrow 0$  in (A.4) one obtains the analytically continued 3-point Witten diagram

$$\frac{1}{\kappa_0} \int_0^\infty \frac{du}{u^2} \int_C dz K_{h_1}(\mathbf{x}, w_1) K_{h_2}(\mathbf{x}, w_2) K_{h_3}(\mathbf{x}, w_3) = \langle \mathcal{O}_{h_1}(w_1) \mathcal{O}_{h_2}(w_2) \mathcal{O}_{h_3}(w_3) \rangle, \quad (\text{A.5})$$

where  $w_i \in \mathbb{C}$  and  $\operatorname{Re}(w_i) \neq \operatorname{Re}(w_j)$  for any  $i \neq j$ .

**Special weights.** In the case when  $h_1 = h_2 + h_3 + 2n$ ,  $n \in \mathbb{N}_0$  and  $h_2, h_3 \in \mathbb{N}$ , the 3-point Witten diagram (4.6) diverges, i.e. it cannot represent the 3-point conformal correlation function. In this case, one uses the following integral representation of the 3-point conformal correlation function that can be checked by calculating both contour integrals on the right-hand side:

$$\begin{aligned} & \langle \mathcal{O}_{h_1}(w_1) \mathcal{O}_{h_2}(w_2) \mathcal{O}_{h_3}(w_3) \rangle \\ &= \frac{\gamma_{h_1 h_2 h_3}}{\alpha'_{h_2 h_3, n}} \frac{1}{(2\pi i)^2} \oint_{u=0} \frac{du}{u^2} \oint_{z=w_1+iu} dz K_{h_1}(\mathbf{x}, w_1) K_{h_2}(\mathbf{x}, w_2) K_{h_3}(\mathbf{x}, w_3), \end{aligned} \quad (\text{A.6})$$

where  $\mathbf{x} = (u, z)$ , the  $\alpha'$ -coefficient is given by (4.22),  $\gamma_{h_1 h_2 h_3}$  is the structure constant (4.3), and  $w_i \in \mathbb{C}$ ,  $\operatorname{Re}(w_i) \neq \operatorname{Re}(w_j)$  for any  $i \neq j$ .

In the case when  $h_1 = h_2 + h_3 + 2n$ ,  $n \in \mathbb{N}_0$  and  $h_2, h_3 \in \mathbb{R}$ , the formula (A.6) can be analytically continued as follows

$$\begin{aligned} & \langle \mathcal{O}_{h_1}(w_1) \mathcal{O}_{h_2}(w_2) \mathcal{O}_{h_3}(w_3) \rangle \\ &= \frac{\gamma_{h_1 h_2 h_3}}{\alpha'_{h_2 h_3, n}} \frac{1}{8\pi^2 i} \frac{(-)^{h_2+h_3}}{\sin(2\pi h_1)} \oint_{u=0} \frac{du}{u^2} \oint_{P[w_1+iu, w_1-iu]} dz K_{h_1}(\mathbf{x}, w_1) K_{h_2}(\mathbf{x}, w_2) K_{h_3}(\mathbf{x}, w_3), \end{aligned} \quad (\text{A.7})$$

where  $P[w_1 + iu, w_1 - iu]$  is the Pochhammer contour around the points  $w_1 \pm iu$ , see fig. 4.

## B Proofs of lemmas

### B.1 Lemma 1

To prove the conversion identity we explicitly calculate the integral in the right-hand side of (4.13), which we call the reconstructed propagator,

$$\int_{z'-iu'}^{z'+iu'} dw \hat{G}_h(\mathbf{x}, \mathbf{x}', w) \equiv G_h^{\text{rec}}(\mathbf{x}, \mathbf{x}'), \quad (\text{B.1})$$

where  $\hat{G}_h(\mathbf{x}, \mathbf{x}', w)$  is given in (3.5), and then show that it coincides with the bulk-to-bulk propagator. Substituting  $\hat{G}_h(\mathbf{x}, \mathbf{x}', w)$  into (B.1) one obtains

$$G_h^{\text{rec}}(\mathbf{x}, \mathbf{x}') = \frac{-2i}{4^h} \frac{\Gamma(2h)}{\Gamma(h)\Gamma(h)} \int_{z'-iu'}^{z'+iu'} dw u'^{1-h} u^h (u'^2 + (z' - w)^2)^{h-1} (u^2 + (z - w)^2)^{-h}. \quad (\text{B.2})$$

Making the change  $w = z' + iu'(2t - 1)$  one obtains

$$\begin{aligned}
G_h^{\text{rec}}(\mathbf{x}, \mathbf{x}') &= \frac{\Gamma(2h)}{\Gamma(h)\Gamma(h)} \left( \frac{uu'}{(u' + u + i(z - z'))(u' - u + i(z - z'))} \right)^h \\
&\times \int_0^1 dt t^{h-1} (1-t)^{h-1} \left( 1 - t \frac{2u'}{u + u' + i(z - z')} \right)^{-h} \left( 1 - t \frac{2u'}{u' - u + i(z - z')} \right)^{-h} \\
&= \left( \frac{uu'}{(u + u' + i(z - z'))(u' - u + i(z - z'))} \right)^h \\
&\times F_1 \left[ \begin{matrix} h, h, h \\ 2h \end{matrix} ; \frac{2u'}{u' + u + i(z - z')}, \frac{2u'}{u' - u + i(z - z')} \right], \tag{B.3}
\end{aligned}$$

where we used the integral representation of the first Appell function [70]

$$F_1 \left[ \begin{matrix} a, b_1, b_2 \\ c \end{matrix} ; z_1, z_2 \right] = \frac{\Gamma(c)}{\Gamma(a)\Gamma(c-a)} \int_0^1 dx x^{a-1} (1-x)^{c-a-1} (1-z_1 x)^{-b_1} (1-z_2 x)^{-b_2}. \tag{B.4}$$

Here,  $z_1, z_2 \in \mathbb{C} \setminus [1, \infty)$  that in (B.3) is equivalent to imposing the following restrictions:

$$\text{Re}(z) \neq \text{Re}(z') \quad \text{or} \quad u > u' - |\text{Im}(z - z')|, \quad \text{where } u, u' \in \mathbb{R}_+ \text{ and } z, z' \in \mathbb{C}. \tag{B.5}$$

Using the following identity [70]

$$F_1 \left[ \begin{matrix} a, b_1, b_2 \\ c \end{matrix} ; z_1, z_2 \right] = (1-z_1)^{-a} F_1 \left[ \begin{matrix} a, c-b_1-b_2, b_2 \\ c \end{matrix} ; \frac{z_1}{z_1-1}, \frac{z_1-z_2}{z_1-1} \right], \tag{B.6}$$

one obtains that the reconstructed propagator is the standard bulk-to-bulk propagator:

$$\begin{aligned}
G_h^{\text{rec}}(\mathbf{x}, \mathbf{x}') &= \left( \frac{uu'}{(u + u')^2 + (z - z')^2} \right)^h F_1 \left[ \begin{matrix} h, h, 0 \\ 2h \end{matrix} ; \frac{4uu'}{(u + u')^2 + (z - z')^2}, \frac{2u'}{u' + u - i(z - z')} \right] \\
&= \left( \frac{\xi(\mathbf{x}, \mathbf{x}')}{2} \right)^h {}_2F_1 \left( \frac{h}{2}, \frac{h}{2} + \frac{1}{2}; h + \frac{1}{2} \middle| \xi(\mathbf{x}, \mathbf{x}')^2 \right) = G_h(\mathbf{x}, \mathbf{x}'), \tag{B.7}
\end{aligned}$$

where  $\xi(\mathbf{x}, \mathbf{x}')$  is defined in (2.7). Here, we used that the first Appell function in (B.7) becomes the Gauss hypergeometric function and then applied the quadratic transformation [70]

$${}_2F_1(a, b; 2a | z) = \left( 1 - \frac{z}{2} \right)^{-b} {}_2F_1 \left( \frac{b}{2}, \frac{b}{2} + \frac{1}{2}; a + \frac{1}{2} \middle| \frac{z^2}{(2-z)^2} \right), \tag{B.8}$$

to obtain the bulk-to-bulk propagator (2.7). This proves Lemma 1.

## B.2 Lemma 2

Let us consider the integral on the left-hand side of (4.19):

$$R(\mathbf{x}_i, \varepsilon) \equiv \int_{z_i - iu_i}^{z_i + iu_i} dw \int_0^\infty \frac{du}{u^2} \int_{C_i(\varepsilon)} dz \widehat{G}_{h_i}(\mathbf{x}, \mathbf{x}_i, w) f(\mathbf{x}), \tag{B.9}$$

where  $\varepsilon \rightarrow 0$  and the contour  $C_i(\varepsilon)$  is shown in fig. 6. Everywhere below we assume that a test function  $f(\mathbf{x})$  is holomorphic on a domain  $U \times V \subset \mathbb{C}^2$ , such that  $U \subset \mathbb{R}$  and  $V \subset C_i(\varepsilon)$  for any  $\varepsilon \rightarrow 0$ . We also assume that the integrand in (B.9) is finite at  $u = 0$  for  $\forall z \in C_i(\varepsilon)$  that restricts  $f(\mathbf{x})$  as follows:  $u^{-h_i} f(\mathbf{x}) = \mathcal{O}(u)$  at  $u \rightarrow 0$ .<sup>11</sup>

Splitting the integration contour  $C_i(\varepsilon)$  into three line segments one obtains

$$\begin{aligned} R(\mathbf{x}_i, \varepsilon) &= \int_{z_i - iu_i}^{z_i + iu_i} dw \int_0^\infty \frac{du}{u^2} \int_{w_i - \varepsilon}^{w_i + \varepsilon} dz \widehat{G}_{h_i}(\mathbf{x}, \mathbf{x}_i, w) f(\mathbf{x}) \\ &+ \int_{z_i - iu_i}^{z_i + iu_i} dw \int_0^\infty \frac{du}{u^2} \int_{z_i - \varepsilon}^{w_i - \varepsilon} dz \widehat{G}_{h_i}(\mathbf{x}, \mathbf{x}_i, w) f(\mathbf{x}) \\ &- \int_{z_i - iu_i}^{z_i + iu_i} dw \int_0^\infty \frac{du}{u^2} \int_{z_i + \varepsilon}^{w_i + \varepsilon} dz \widehat{G}_{h_i}(\mathbf{x}, \mathbf{x}_i, w) f(\mathbf{x}). \end{aligned} \quad (\text{B.10})$$

The first term is proportional to  $\varepsilon$  because a length of the contour equals  $2\varepsilon$  and the integrand is holomorphic in the integration domain. Then, by changing  $z$  to  $z' = z \pm \varepsilon$  in the second and third lines one represents (B.10) up to  $\mathcal{O}(\varepsilon)$  terms as follows

$$R(\mathbf{x}_i, \varepsilon) = \int_{z_i - iu_i}^{z_i + iu_i} dw \int_0^\infty \frac{du}{u^2} \int_{z_i}^{w_i} dz (\widehat{G}_{h_i}(z - \varepsilon, u, \mathbf{x}_i, w) - \widehat{G}_{h_i}(z + \varepsilon, u, \mathbf{x}_i, w)) f(\mathbf{x}) + \mathcal{O}(\varepsilon), \quad (\text{B.11})$$

where: (1) we took into account that  $f(\mathbf{x})$  is holomorphic; (2) we expanded  $f(u, z' \pm \varepsilon)$  into the Taylor series around  $\mathbf{x} = (u, z')$ ; (3) we omitted terms linear in  $\varepsilon$ ; (4) we renamed  $z' \rightarrow z$ , for convenience. The integrand is a test function times a discontinuity of the modified propagator.

Before calculating (B.11) explicitly, let us find domains of  $z, u, w$  where the discontinuity is non-vanishing. Using the modified propagator (3.5) and the following relation

$$(x + i\varepsilon)^\alpha - (x - i\varepsilon)^\alpha = \theta(-x)(e^{\pi i \alpha} - e^{-\pi i \alpha})(x + i\varepsilon)^\alpha + \mathcal{O}(\varepsilon), \quad \alpha \in \mathbb{R}, \quad (\text{B.12})$$

one finds that

$$\begin{aligned} \text{Disc}(\widehat{G}_{h_i}(z \mp \varepsilon, u, \mathbf{x}_i, w)) &= \widehat{G}_{h_i}(z - \varepsilon, u, \mathbf{x}_i, w) - \widehat{G}_{h_i}(z + \varepsilon, u, \mathbf{x}_i, w) \\ &= \text{sign}(iz - iw) \theta((iz - iw)^2 - u^2)(e^{-\pi i h_i} - e^{\pi i h_i}) \widehat{G}_{h_i}(z + \varepsilon, u, \mathbf{x}_i, w) + \mathcal{O}(\varepsilon), \end{aligned} \quad (\text{B.13})$$

where the sign function is defined as  $\text{sign}(x) = 2\theta(x) - 1$ . Here,  $iz - iw \in \mathbb{R}$ , which follows from the integration domains of  $w$  and  $z$  in (B.11), ensuring that arguments of the sign and step functions are real. The resulting restriction on  $z, u, w$  is given by the step function in (B.13), i.e.  $(iz - iw)^2 - u^2 \geq 0$ .

Returning to the integral (B.11), one substitutes  $\widehat{G}_{h_i}(\mathbf{x}, \mathbf{x}_i, w)$  (3.5), takes into account the restriction  $(iz - iw)^2 - u^2 \geq 0$  for  $u$  and  $z$  (otherwise the integrand is zero), makes the

---

<sup>11</sup>In the case when a test function is chosen to be a product of two bulk-to-bulk propagators,  $f(\mathbf{x}) = G_{h_j}(\mathbf{x}, x_j) G_{h_k}(\mathbf{x}, x_k)$ ,  $i \neq j \neq k \neq i$ , this restriction is equivalent to the triangle inequality  $h_j + h_k > h_i$ .

change  $z = z_i + iv$ ,  $w = z_i + it$ , and then interchanges integrations over  $t$  and  $v$ :

$$\begin{aligned} R(\mathbf{x}_i, \varepsilon) &= \frac{2i}{4^{h_i}} \frac{\Gamma(2h_i)}{\Gamma(h_i)\Gamma(h_i)} u_i^{1-h_i} \int_0^{u_i} \frac{du}{u^2} u^{h_i} \int_0^{u_i-u} dv (I_1(u, v, \varepsilon) - I_1(u, v, -\varepsilon)) f(z_i + iv, u) \\ &\quad - \frac{2i}{4^{h_i}} \frac{\Gamma(2h_i)}{\Gamma(h_i)\Gamma(h_i)} u_i^{1-h_i} \int_0^{u_i} \frac{du}{u^2} u^{h_i} \int_{u-u_i}^0 dv (I_2(u, v, \varepsilon) - I_2(u, v, -\varepsilon)) f(z_i + iv, u) + O(\varepsilon), \end{aligned} \quad (\text{B.14})$$

where

$$\begin{aligned} I_1(u, v, \varepsilon) &= \int_v^{u_i} dt (u_i^2 - t^2)^{h_i-1} (u^2 + (iv - it - \varepsilon)^2)^{-h_i}, \\ I_2(u, v, \varepsilon) &= \int_{-u_i}^v dt (u_i^2 - t^2)^{h_i-1} (u^2 + (iv - it - \varepsilon)^2)^{-h_i}. \end{aligned} \quad (\text{B.15})$$

The integrals are split due to the Heaviside step function and the interchange of the order of integration. Note that the domain of  $t$  is not restricted as the integrals (B.15) are easier to calculate without imposing such a restriction.

Now, we calculate  $I_1(u, v, \varepsilon)$  by changing  $t = v + (u_i - v)s$ ,  $s \in [0, 1]$ , and using the integral representation of the Lauricella function [71]

$$F_D^n \left[ \begin{matrix} a, b_1, \dots, b_n \\ c \end{matrix} ; z_1, \dots, z_n \right] = \frac{\Gamma(c)}{\Gamma(a)\Gamma(c-a)} \int_0^1 dx x^{a-1} (1-x)^{c-a-1} \prod_{i=1}^n (1-z_i x)^{-b_i}. \quad (\text{B.16})$$

The result is

$$\begin{aligned} I_1(u, v, \varepsilon) &= \frac{\Gamma(h_i)}{\Gamma(h_i+1)} \left( \frac{u_i - v}{(u + i\varepsilon)(u - i\varepsilon)} \right)^{h_i} (u_i + v)^{h_i-1} \\ &\quad \times F_D^3 \left[ \begin{matrix} 1, 1-h_i, h_i, h_i \\ h_i+1 \end{matrix} ; \frac{v-u_i}{u_i+v}, \frac{u_i-v}{u+i\varepsilon}, \frac{v-u_i}{u-i\varepsilon} \right]. \end{aligned} \quad (\text{B.17})$$

The Lauricella function on the right-hand side can be transformed by using the following relation [71]

$$\begin{aligned} F_D^3 \left[ \begin{matrix} a, b_1, b_2, b_3 \\ c \end{matrix} ; z_1, z_2, z_3 \right] \\ = (1-z_3)^{-a} F_D^3 \left[ \begin{matrix} a, b_1, b_2, c - \sum_{i=1}^3 b_i \\ c \end{matrix} ; \frac{z_1-z_3}{1-z_3}, \frac{z_2-z_3}{1-z_3}, \frac{z_3}{z_3-1} \right], \end{aligned} \quad (\text{B.18})$$

where we note that  $c, b_i$  in (B.17) satisfy  $c - \sum_{i=1}^3 b_i = 0$ , and, therefore, the Lauricella function reduces to the first Appell function,

$$\begin{aligned} I_1(u, v, \varepsilon) &= \frac{\Gamma(h_i)}{\Gamma(h_i+1)} \left( \frac{u_i - v}{u + i\varepsilon} \right)^{h_i} \left( \frac{u_i + v}{u - i\varepsilon} \right)^{h_i-1} (u + u_i - v - i\varepsilon)^{-1} \\ &\quad \times F_1 \left[ \begin{matrix} 1, 1-h_i, h_i \\ h_i+1 \end{matrix} ; \frac{u_i - v}{u_i + v}, \frac{u_i - u + v + i\varepsilon}{u_i + u - v - i\varepsilon}, \frac{2u_i(u_i - v)}{(u + i\varepsilon)(u_i + u - v - i\varepsilon)} \right]. \end{aligned} \quad (\text{B.19})$$

In order to find  $I_1(u, v, \varepsilon) - I_1(u, v, -\varepsilon)$  at  $\varepsilon \rightarrow 0$  one studies the analytical properties of the function  $I_1(u, v, \varepsilon)$ . The prefactor in (B.19) is a continuous function of  $\varepsilon$  at  $\varepsilon \rightarrow 0^\pm$  for  $u \leq u_i$  and  $0 \leq v \leq u_i - u$  because the real parts of the arguments of all power functions are greater than zero. The only source of discontinuity in  $I_1(u, v, \varepsilon)$  is the first Appell function  $F_1 \left[ \begin{matrix} a, b_1, b_2 \\ c \end{matrix}; z_1, z_2 \right]$ , which has two branch cuts  $\text{Re}(z_1) > 1$ ,  $\text{Im}(z_1) = 0$  and  $\text{Re}(z_2) > 1$ ,  $\text{Im}(z_2) = 0$ . In our case, the restrictions on  $u$  and  $v$  arising from the integration domain constrain the arguments of the first Appell function as follows

$$\begin{aligned} z_1 &= \frac{u_i - v}{u_i + v} \frac{u_i - u + v + i\varepsilon}{u_i + u - v - i\varepsilon}, \quad |z_1| \leq 1; \\ z_2 &= \frac{2u_i(u_i - v)}{(u + i\varepsilon)(u_i + u - v - i\varepsilon)}, \quad 2 > \text{Re } z_2 \geq 1, \text{Im } z_2 \sim \varepsilon, |1 - z_2| < 1, \end{aligned} \quad (\text{B.20})$$

i.e. the discontinuity of  $I_1(u, v, \varepsilon)$  is proportional to the discontinuity of the first Appell function at the branch cut  $\text{Re}(z_2) > 1$ ,  $\text{Im}(z_2) = 0$ .

The discontinuity can be found by using the following expansion of the first Appell function at  $|z_1| < 1$  and  $|1 - z_2| < 1$  [72]:

$$\begin{aligned} F_1 \left[ \begin{matrix} a, b_1, b_2 \\ a + b_2 \end{matrix}; z_1, z_2 \right] &= -\frac{\Gamma(a + b_2)}{\Gamma(a)\Gamma(b_2)} \sum_{k=0}^{\infty} \frac{(a)_k (b_2)_k}{k!k!} (1 - z_2)^k \left[ \frac{d}{ds} {}_2F_1(b_1, a + s, a, z_1) \right]_{s=k} \\ &+ \ln(1 - z_2) {}_2F_1(b_1, a + k, a, z_1) - h_k^+(b_2, a) {}_2F_1(b_1, a + k, a, z_1) \Big]. \end{aligned} \quad (\text{B.21})$$

Here,  $h_k^+(b_2, a)$  is some function of  $b_2, a$ , and  $k$ , whose form is irrelevant for calculating the discontinuity because the term in (B.21) containing  $h_k^+(b_2, a)$  is a holomorphic function of  $z_1$  and  $z_2$  in the domain  $|1 - z_2| < 1$  and  $|z_1| < 1$ . The same applies to the first line in (B.21). The only term contributing to the discontinuity is that one containing the logarithm. Substituting (B.21) into  $I_1(u, v, \varepsilon) - I_1(u, v, -\varepsilon)$  one obtains

$$\begin{aligned} I_1(u, v, \varepsilon) - I_1(u, v, -\varepsilon) &= 2i\pi \left( \frac{u_i - v}{u} \right)^{h_i} \left( \frac{u_i + v}{u} \right)^{h_i-1} (u + u_i - v)^{-1} \\ &\times {}_2F_2 \left[ \begin{matrix} 1, h_i, 1 - h_i \\ 1, 1 \end{matrix}; \frac{-u_i + u + v}{u_i + u - v}, \frac{u_i - v}{u_i + v} \frac{u_i - u + v}{u_i + u - v} \right] + O(\varepsilon), \end{aligned} \quad (\text{B.22})$$

where we summed the discontinuity of (B.21) over  $k$  to obtain the second Appell function, which can be further simplified using two identities [70]:

$$\begin{aligned} F_1 \left[ \begin{matrix} a, b_1, b_2 \\ a, a \end{matrix}; z_1, z_2 \right] &= (1 - z_1)^{-b_1} (1 - z_2)^{-b_2} {}_2F_1 \left( \begin{matrix} b_1, b_2 \\ a \end{matrix}; a \left| \frac{z_1 z_2}{(1 - z_1)(1 - z_2)} \right. \right), \\ {}_2F_1 \left( \begin{matrix} a, 1 - a \\ c \end{matrix}; c \left| z \right. \right) &= (1 - z)^{c-1} (1 - 2z)^{a-c} {}_2F_1 \left( \begin{matrix} c - a, c - a + 1 \\ 2, 2 \end{matrix}; c \left| \frac{4z(1 - z)}{(1 - 2z)^2} \right. \right). \end{aligned} \quad (\text{B.23})$$

The resulting expression is given by

$$\begin{aligned} & I_1(u, v, \varepsilon) - I_1(u, v, -\varepsilon) \\ &= i\pi u^{-h_i} u_i^{h_i-1} \xi(\mathbf{y}, \mathbf{x}_i)^{1-h_i} {}_2F_1\left(\frac{1}{2} - \frac{h_i}{2}, 1 - \frac{h_i}{2}; 1 \mid 1 - \xi(\mathbf{y}, \mathbf{x}_i)^2\right) + O(\varepsilon), \end{aligned} \quad (\text{B.24})$$

where  $\mathbf{y} = (u, z_i + iv)$  and  $\xi(\mathbf{y}, \mathbf{x}_i)$  is defined in (2.7). Similarly, one finds the discontinuity of  $I_2(u, v, \varepsilon)$ :

$$\begin{aligned} & I_2(u, v, \varepsilon) - I_2(u, v, -\varepsilon) \\ &= -i\pi u^{-h_i} u_i^{h_i-1} \xi(\mathbf{y}, \mathbf{x}_i)^{1-h_i} {}_2F_1\left(\frac{1}{2} - \frac{h_i}{2}, 1 - \frac{h_i}{2}; 1 \mid 1 - \xi(\mathbf{y}, \mathbf{x}_i)^2\right) + O(\varepsilon). \end{aligned} \quad (\text{B.25})$$

By substituting (B.24) and (B.25) into (B.14) one obtains the final relation

$$\begin{aligned} \lim_{\varepsilon \rightarrow 0} R(\mathbf{x}_i, \varepsilon) &= \int_{z_i-iu_i}^{z_i+iu_i} dw \int_0^\infty \frac{du}{u^2} \int_{C_i(\varepsilon)} dz \widehat{G}_{h_i}(\mathbf{x}, \mathbf{x}_i, w) f(\mathbf{x}) \\ &= \pi \int_0^{u_i} \frac{du}{u^2} \int_{z_i-i(u_i-u)}^{z_i+i(u_i-u)} dz \widetilde{G}_{h_i}(\mathbf{x}, \mathbf{x}_i) f(\mathbf{x}), \end{aligned} \quad (\text{B.26})$$

where we used the definition of  $R(\mathbf{x}_i, \varepsilon)$  (B.9), made the change  $v = iz_i - iz$ , and used the modified propagator (3.5). This proves Lemma 2.

### B.3 Lemma 3

Let us consider the integral on the left-hand side of (4.21) with two points taken on the boundary  $\mathbf{x}_1 = (0, z_1)$ ,  $\mathbf{x}_2 = (0, z_2)$ , which is multiplied by the factor  $\frac{4^{h_3}}{-2i} \frac{\Gamma(h_3)\Gamma(h_3)}{\Gamma(2h_3)}$ :

$$\begin{aligned} V(z_1, z_2, \mathbf{x}_3) &\equiv \frac{4^{h_3}}{-2i} \frac{\Gamma(h_3)\Gamma(h_3)}{\Gamma(2h_3)} \frac{1}{8i\pi^3} \frac{(-)^{h_1+h_2}}{\sin(2\pi(h_1+h_2))} \sum_{n=0}^\infty \frac{a(h_3; h_1, h_2; n)}{\alpha'_{h_1 h_2, n}} \\ &\times \int_{z_3-iu_3}^{z_3+iu_3} dw \oint_0 \frac{du}{u^2} \oint_{P[w-iu, w+iu]} dz K_{h_1}(\mathbf{x}, z_1) K_{h_2}(\mathbf{x}, z_2) \widehat{G}_{h_{12|n}}(\mathbf{x}, \mathbf{x}_3, w), \end{aligned} \quad (\text{B.27})$$

where the coefficients  $a(h_3; h_1, h_2; n)$ ,  $\alpha'_{h_1 h_2, n}$  are defined in (2.5), (4.22),  $P[w - iu, w + iu]$  is the Pochhammer contour, see fig. 4,  $K_{h_i}(\mathbf{x}, z_i)$  is the bulk-to-boundary propagator (2.8) and  $\widehat{G}_{h_{12|n}}(\mathbf{x}, \mathbf{x}_3, w)$  is the modified propagator (3.5). In order to prove Lemma 3 one shows that (B.27) coincides (up to the additional factor of  $\frac{4^{h_3}}{-2i} \frac{\Gamma(h_3)\Gamma(h_3)}{\Gamma(2h_3)}$ ) with the left-hand side of (4.21), where two points are taken on the boundary. To this end, we perform a series of transformations including integrations and infinite summations.

Substituting  $a(h_3; h_1, h_2; n)$ ,  $\alpha'_{h_1 h_2, n}$ ,  $K_{h_i}(\mathbf{x}, z_i)$ ,  $\widehat{G}_{h_{12|n}}(\mathbf{x}, \mathbf{x}_3, w)$  and changing  $z = w - iu + 2ius$ ,  $w = z_3 - iu_3 + 2iu_3t$  in (4.21) yields

$$\begin{aligned} V(z_1, z_2, \mathbf{x}_3) = & -\frac{1}{4i\pi^2} \frac{(-)^{h_3}}{\sin(2\pi(h_{12|n}))} \sum_{n=0}^{\infty} \frac{(h_{12|n} - 1)}{(h_{12|n} - h_3)(h_{12|n} + h_3 - 1)} \oint_0 \frac{du}{u} \int_0^1 dt \oint_{P[0,1]} ds \\ & \times (u^2 - (u + u_3 + iz_{13} - 2us - 2u_3t)^2)^{-h_1} (u^2 - (u + u_3 + iz_{23} - 2us - 2u_3t)^2)^{-h_2} \\ & \times (t(1-t))^{h_{12|n}-1} (s(1-s))^{-h_{12|n}} \left(\frac{u_3}{u}\right)^{2n}. \end{aligned} \quad (\text{B.28})$$

To integrate over  $s$  one uses the analytically continued integral representation of the Lauricella function  $F_D^4$ , which is the regular integral representation (B.16), where the integration contour is changed to the Pochhammer contour  $P[0, 1]$ . By expanding the resulting function  $F_D^4$  into a series one obtains

$$\begin{aligned} V(z_1, z_2, \mathbf{x}_3) = & \frac{(-)^{h_3}}{\pi} \sum_{n=0}^{\infty} \frac{\Gamma(2h_{12|n})}{\Gamma(h_{12|n})^2} \frac{(-)^{2h_{12|n}}}{(h_{12|n} - h_3)(h_{12|n} + h_3 - 1)} \\ & \times \oint_0 \frac{du}{u} \int_0^1 dt \sum_{k_1, \dots, k_4=0}^{\infty} \frac{(1 - h_{12|n})_K (h_1)_{k_1} (h_1)_{k_2} (h_2)_{k_3} (h_2)_{k_4}}{(2 - 2h_{12|n})_K k_1! k_2! k_3! k_4!} \\ & \times (t(1-t))^{h_{12|n}-1} u_3^{2n} u^{K-2n} 2^K (2u + u_3 + iz_{13} - 2u_3t)^{-h_1-k_1} \\ & \times (u_3 + iz_{13} - 2u_3t)^{-h_1-k_2} (2u + u_3 + iz_{23} - 2u_3t)^{-h_2-k_3} (u_3 + iz_{23} - 2u_3t)^{-h_2-k_4}, \end{aligned} \quad (\text{B.29})$$

where, for convenience, we denoted  $K = k_1 + k_2 + k_3 + k_4$ , and used the series representation of the Lauricella function,

$$F_D^n \left[ \begin{matrix} a, b_1, \dots, b_n \\ c \end{matrix} ; z_1, \dots, z_n \right] = \sum_{m_1, \dots, m_n=1}^{\infty} \frac{(a)_{\sum_{i=1}^n m_i}}{(c)_{\sum_{i=1}^n m_i}} \prod_{i=1}^n (b_i)_{m_i} \frac{z_i^{m_i}}{m_i!}, \quad |z_i| < 1. \quad (\text{B.30})$$

To integrate over  $t$  one again uses the integral representation of the Lauricella function  $F_D^4$  and expands it into a series,

$$\begin{aligned} V(z_1, z_2, \mathbf{x}_3) = & \frac{(-)^{h_3}}{\pi} \sum_{n=0}^{\infty} \frac{(-)^{2h_{12|n}}}{(h_{12|n} - h_3)(h_{12|n} + h_3 - 1)} \oint_0 \frac{du}{u} \sum_{\substack{k_1, \dots, k_4=0 \\ l_1, \dots, l_4=0}}^{\infty} \frac{(h_{12|n})_L}{(2h_{12|n})_L} \\ & \times \frac{(1 - h_{12|n})_K}{(2 - 2h_{12|n})_K} \frac{(h_1)_{k_1+l_1} (h_1)_{k_2+l_2} (h_2)_{k_3+l_3} (h_2)_{k_4+l_4}}{k_1! k_2! k_3! k_4! l_1! l_2! l_3! l_4!} 2^{K+L} u^{K-2n} u_3^{L+2n} \\ & \times (2u + u_3 + iz_{13})^{-h_1-k_1-l_1} (u_3 + iz_{13})^{-h_1-k_2-l_2} (2u + u_3 + iz_{23})^{-h_2-k_3-l_3} (u_3 + iz_{23})^{-h_2-k_4-l_4}, \end{aligned} \quad (\text{B.31})$$

where we denoted  $L = l_1 + l_2 + l_3 + l_4$ . Note that the convergence of the infinite sums here is guaranteed by the following restrictions on  $z_{13}$  and  $z_{23}$ :  $|z_{13}| > 2u_3$  and  $|z_{23}| > 2u_3$ .

The next step is to sum over  $n$ . By imposing the restriction  $|u| > u_3$  on the integration contour in the integral over  $u$ , which can be achieved by continuous contour deformation, we

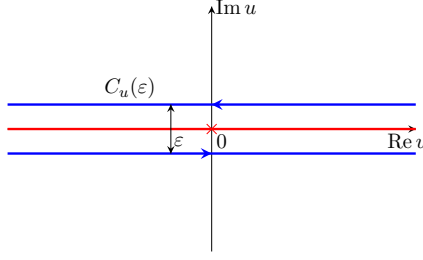


**Figure 10.** The contour  $C_u$  on the complex  $u$ -plane. The red cross and the red line are respectively the singularity and the branch cut of the integrand (B.33); the regularization parameter  $\varepsilon \rightarrow 0$ .

ensure that after the change of order of the summation over  $n$  and the integration over  $u$  the infinite sum over  $n$  converges. This sum is in fact the hypergeometric function  ${}_10F_9$ , which we then represent as the Mellin-Barnes integral using the following identity

$$\begin{aligned}
 {}_pF_q(a_1, \dots, a_p; b_1, \dots, b_q | x) &= \sum_{n=0}^{\infty} \frac{(a_1)_n \dots (a_p)_n}{(b_1)_n, \dots, (b_q)_n} \frac{x^n}{n!} \\
 &= \frac{1}{2i\pi} \frac{\Gamma(b_1) \dots \Gamma(b_q)}{\Gamma(a_1) \dots \Gamma(a_p)} \int_{-i\infty}^{i\infty} dc \frac{\Gamma(a_1 + c) \dots \Gamma(a_p + c) \Gamma(-c)}{\Gamma(b_1 + c) \dots \Gamma(b_q + c)} (-x)^c.
 \end{aligned} \tag{B.32}$$

The resulting expression takes the form

$$\begin{aligned}
 V(z_1, z_2, \mathbf{x}_3) &= \frac{(-)^{h_3-2h_2-2h_3}}{2i\pi^2} \oint_{|u|>u_3} \frac{du}{u} \int_{-i\infty}^{i\infty} dc \frac{\Gamma(-c)\Gamma(c+1)}{(h_{12|c}-h_3)(h_{12|c}+h_3-1)} \\
 &\times \sum_{\substack{k_1, \dots, k_4=0 \\ l_1, \dots, l_4=0}}^{\infty} \frac{(h_{12|c})_L}{(2h_{12|c})_L} \frac{(1-h_{12|c})_K}{(2-2h_{12|c})_K} \frac{(h_1)_{k_1+l_1} (h_1)_{k_2+l_2} (h_2)_{k_3+l_3} (h_2)_{k_4+l_4}}{k_1! k_2! k_3! k_4! l_1! l_2! l_3! l_4!} 2^{K+L} u^K u_3^L \left(-\frac{u_3^2}{u^2}\right)^c \\
 &\times (2u + u_3 + iz_{13})^{-h_1-k_1-l_1} (u_3 + iz_{13})^{-h_1-k_2-l_2} (2u + u_3 + iz_{23})^{-h_2-k_3-l_3} (u_3 + iz_{23})^{-h_2-k_4-l_4}.
 \end{aligned} \tag{B.33}$$

To simplify the integral over  $u$  one replaces the integration contour by the contour  $C_u(\varepsilon)$  shown in fig. 10. This change allows one to rewrite the integral over  $u$  as a difference of two integrals, and, therefore, as the integral over the discontinuity of the integrand. A similar procedure was performed when proving Lemma 2, see (B.10) and (B.11). Repeating this procedure, calculating the discontinuity of the factor  $\left(-\frac{u_3^2}{u^2}\right)^c$  using (B.12), taking the limit  $\varepsilon \rightarrow 0$  and showing that at  $|u| > u_3$  the Mellin-Barnes integral is zero, one obtains

$$\begin{aligned}
 V(z_1, z_2, \mathbf{x}_3) &= -\frac{(-)^{h_1-2h_2-2h_3}}{i\pi} \int_0^{u_3} \frac{du}{u} \int_{-i\infty}^{i\infty} dc \frac{1}{(h_{12|c}-h_3)(h_{12|c}+h_3-1)} \\
 &\times \sum_{\substack{k_1, \dots, k_4=0 \\ l_1, \dots, l_4=0}}^{\infty} \frac{(h_{12|c})_L}{(2h_{12|c})_L} \frac{(1-h_{12|c})_K}{(2-2h_{12|c})_K} \frac{(h_1)_{k_1+l_1} (h_1)_{k_2+l_2} (h_2)_{k_3+l_3} (h_2)_{k_4+l_4}}{k_1! k_2! k_3! k_4! l_1! l_2! l_3! l_4!} 2^{K+L} u^{K-2c} u_3^{L+2c}
 \end{aligned} \tag{B.34}$$

$$\times (2u + u_3 + iz_{13})^{-h_1 - k_1 - l_1} (u_3 + iz_{13})^{-h_1 - k_2 - l_2} (2u + u_3 + iz_{23})^{-h_2 - k_3 - l_3} (u_3 + iz_{23})^{-h_2 - k_4 - l_4},$$

where we also used that the integrand is even function of  $u$ . Making the change  $l_i = n_i - k_i$ ,  $k_1 = K_1 - k_2 - k_3 - k_4$  and summing over  $k_2, k_3, k_4$  by means of the following identity [70]

$$\sum_{k=0} \frac{(a)_k (b)_k}{k! (c)_k} = \frac{\Gamma(c) \Gamma(c-a-b)}{\Gamma(c-a) \Gamma(c-b)}, \quad \text{Re}(c-a-b) > 0, \quad (\text{B.35})$$

one obtains

$$\begin{aligned} V(z_1, z_2, \mathbf{x}_3) = & -\frac{(-)^{h_1-2h_2-2h_3}}{i\pi} \int_0^{u_3} \frac{du}{u} \int_{-i\infty}^{i\infty} dc \frac{1}{(h_{12|c} - h_3)(h_{12|c} + h_3 - 1)} \\ & \times \sum_{n_1, \dots, n_4=0}^{\infty} \frac{(h_1)_{n_1} (h_1)_{n_2} (h_2)_{n_3} (h_2)_{n_4}}{n_1! n_2! n_3! n_4!} \sum_{K_1=0}^N \frac{(1-h_{12|c})_N (h_{12|c})_{N-K_1}}{(2-2h_{12|c})_{K_1} (2h_{12|c})_{N-K_1}} \frac{(N)!}{K_1! (N-K_1)!} \\ & \times 2^N u^{K_1-2c} u_3^{N-K_1+2c} (2u + u_3 + iz_{13})^{-h_1-n_1} (u_3 + iz_{13})^{-h_1-n_2} \\ & \times (2u + u_3 + iz_{23})^{-h_2-n_3} (u_3 + iz_{23})^{-h_2-n_4}, \end{aligned} \quad (\text{B.36})$$

where  $N = n_1 + n_2 + n_3 + n_4$ . Applying the following identity to the sum over  $K_1$  [70]

$$\sum_{k=0}^{\infty} \frac{(a)_k (b)_k (c)_k}{k! (a-b+1)_k (a-c+1)_k} z^k = (1-z)^{-a} \sum_{k=0}^{\infty} \frac{(a-b-c+1)_k (\frac{a}{2})_k (\frac{a}{2} + \frac{1}{2})_k}{k! (a-b+1)_k (a-c+1)_k} \left( -\frac{4z}{(1-z)^2} \right)^k, \quad (\text{B.37})$$

where  $|z| < 1$  and  $|\frac{4z}{(1-z)^2}| < 1$ , one obtains

$$\begin{aligned} V(z_1, z_2, \mathbf{x}_3) = & -\frac{(-)^{h_1-2h_2-2h_3}}{i\pi} \int_0^{u_3} \frac{du}{u} \int_{-i\infty}^{i\infty} dc \frac{1}{(h_{12|c} - h_3)(h_{12|c} + h_3 - 1)} \\ & \times \sum_{n_1, \dots, n_4, K_1=0}^{\infty} \frac{(h_1)_{n_1} (h_1)_{n_2} (h_2)_{n_3} (h_2)_{n_4}}{K_1! n_1! n_2! n_3! n_4!} \frac{(1-h_{12|c})_N (h_{12|c})_{N-K_1}}{(2-2h_{12|c})_{K_1} (2h_{12|c})_{N-2K_1}} (-)^{K_1} \\ & \times 2^N u^{K_1-2c} u_3^{1-h_{12|c}+K_1} (u_3 + u)^{2h_{12|c}+N-2K_1-1} (2u + u_3 + iz_{13})^{-h_1-n_1} (u_3 + iz_{13})^{-h_1-n_2} \\ & \times (2u + u_3 + iz_{23})^{-h_2-n_3} (u_3 + iz_{23})^{-h_2-n_4}. \end{aligned} \quad (\text{B.38})$$

Now, using (B.30) and (B.16), one rewrites the sums over  $n_i$  as the integral over  $v$ :

$$\begin{aligned} V(z_1, z_2, \mathbf{x}_3) = & \frac{1}{i\pi} \int_0^{u_3} \frac{du}{u} \sum_{K=0}^{\infty} \int_{-i\infty}^{i\infty} dc \left( \frac{v(1-v)(u_3+u)^2}{uu_3} \right)^{2c} \frac{u^K u_3^{1-h_1-h_2+K} (h_{12|c} - 1)}{(h_{12|c} - h_3)(h_{12|c} + h_3 - 1)} \\ & \frac{(u_3+u)^{2h_1+2h_2-1-2K}}{K! \Gamma(h_{12|c} - K)^2 \Gamma(2-2h_{12|c} + K)} \int_0^1 dv (v(1-v))^{h_1+h_2-K-1} \\ & \times (u^2 - (u + u_3 + iz_{13} - 2v(u + u_3))^2)^{-h_1} (u^2 - (u + u_3 + iz_{23} - 2v(u + u_3))^2)^{-h_2}. \end{aligned} \quad (\text{B.39})$$

To calculate the Mellin-Barnes integral over  $c$  one notes that it should be closed to the left, otherwise the integral is zero as there are no poles to the right of the contour. This leads to the restriction  $v(1-v)(u_3+u)^2 \geq uu_3$ , which is equivalent to restricting the integration domain in the second integral:  $v \in [\frac{u}{u+u_3}, \frac{u_3}{u+u_3}]$ . Closing the contour to the left, one calculates the residues of simple poles located at  $2c = h_1 - h_2 - h_3$  and  $2c = 1 - h_1 - h_2 - h_3$ , makes the change  $v = \frac{u_3+u-iz+iz_3}{2(u+u_3)}$  and then sums over  $K_1$ :

$$V(z_1, z_2, \mathbf{x}_3) = \int_0^{u_3} \frac{du}{u^2} u^{h_1+h_2} \int_{z_3-i(u_3-u)}^{z_3+i(u_3-u)} dz (u^2 + (z_1 - z)^2)^{-h_1} (u^2 + (z_2 - z)^2)^{-h_2} \\ \times \left[ \frac{\Gamma(2h_3 - 1)}{\Gamma(h_3)^2} \left( \frac{4uu_3}{(u+u_3)^2 + (z_3 - z)^2} \right)^{1-h_3} {}_2F_1 \left( 1 - h_3, 1 - h_3; 2 - 2h_3 \middle| \frac{4uu_3}{(u+u_3)^2 + (z_3 - z)^2} \right) \right. \\ \left. + \frac{\Gamma(1 - 2h_3)}{\Gamma(1 - h_3)^2} \left( \frac{4uu_3}{(u+u_3)^2 + (z_3 - z)^2} \right)^{h_3} {}_2F_1 \left( h_3, h_3; 2h_3 \middle| \frac{4uu_3}{(u+u_3)^2 + (z_3 - z)^2} \right) \right]. \quad (\text{B.40})$$

The sum of hypergeometric functions in the last two lines can be transformed into a single hypergeometric function using the following identity [70]

$$\frac{\Gamma(2a - 1)}{\Gamma(a)^2} x^{1-a} {}_2F_1 \left( 1 - a, 1 - a; 2 - 2a \middle| x \right) + x^a \frac{\Gamma(1 - 2a)}{\Gamma(1 - a)^2} {}_2F_1 \left( a, a; 2a \middle| x \right) \\ = x^a {}_2F_1 \left( a, a; 1 \middle| 1 - x \right) = - \left( \frac{x}{2 - x} \right)^{1-a} {}_2F_1 \left( 1 - \frac{a}{2}, \frac{1}{2} - \frac{a}{2}; 1 \middle| \frac{4(1-x)}{(2-x)^2} \right), \quad (\text{B.41})$$

where we also used the quadratic identity in the last line. Using (B.41) in (B.40) yields

$$V(z_1, z_2, \mathbf{x}_3) = \int_0^{u_3} \frac{du}{u^2} u^{h_1+h_2} \int_{z_3-i(u-u_3)}^{z_3+i(u-u_3)} dz (u^2 + (z_1 - z)^2)^{-h_1} (u^2 + (z_2 - z)^2)^{-h_2} \\ \times \left( \frac{2uu_3}{u^2 + u_3^2 + (z_3 - z)^2} \right)^{1-h_3} {}_2F_1 \left( 1 - \frac{h_3}{2}, \frac{1}{2} - \frac{h_3}{2}; 1 \middle| 1 - \left( \frac{2uu_3}{u^2 + u_3^2 + (z_3 - z)^2} \right)^2 \right) \\ = \frac{4^{h_3}}{-2i} \frac{\Gamma(h_3)\Gamma(h_3)}{\Gamma(2h_3)} \int_0^{u_3} \frac{du}{u^2} \int_{z_3-i(u-u_3)}^{z_3+i(u-u_3)} dz K_{h_1}(\mathbf{x}, z_1) K_{h_2}(\mathbf{x}, z_2) \tilde{G}_{h_3}(\mathbf{x}, \mathbf{x}_3), \quad (\text{B.42})$$

where we used the modified propagator  $\tilde{G}_{h_3}(\mathbf{x}, \mathbf{x}_3)$  (3.5)

$$\tilde{G}_h(\mathbf{x}, \mathbf{x}') = \frac{-2i}{4^h} \frac{\Gamma(2h)}{\Gamma(h)\Gamma(h)} \left( \frac{\Gamma(1-2h)}{\Gamma(1-h)^2} G_h(\mathbf{x}, \mathbf{x}') + \frac{\Gamma(2h-1)}{\Gamma(h)^2} G_{1-h}(\mathbf{x}, \mathbf{x}') \right) \\ = \frac{-2i}{4^h} \frac{\Gamma(2h)}{\Gamma(h)\Gamma(h)} \xi(\mathbf{x}, \mathbf{x}')^{1-h} {}_2F_1 \left( 1 - \frac{h}{2}, \frac{1}{2} - \frac{h}{2}; 1 \middle| 1 - \xi(\mathbf{x}, \mathbf{x}')^2 \right). \quad (\text{B.43})$$

This proves the Lemma 3 in the case when the points  $\mathbf{x}_1$  and  $\mathbf{x}_2$  are located on the boundary. In the case when these points are in the bulk, one multiplies the relation (B.42) by two smearing functions  $\mathbb{K}_{h_1}(\mathbf{x}_1, w_1)$ ,  $\mathbb{K}_{h_2}(\mathbf{x}_2, w_2)$  (2.3), integrates over the boundary points  $w_1$ ,

$w_2$  and uses the conversion identity (4.13), which turns the bulk-to-boundary propagators in (B.42) into the bulk-to-bulk propagators. These steps provide the final proof of Lemma 3. Also note that the restrictions  $|z_{13}| > 2u_3$  and  $|z_{23}| > 2u_3$  imposed on  $z_1, z_2, z_3$  can be lifted by means of analytic continuation, as both sides of the identity (B.42) are well-defined in the domain  $|z_{13}| < 2u_3$  and  $|z_{23}| < 2u_3$  as long as  $z_i \neq z_j, \forall i \neq j$ .

Note that the right-hand side of (4.21) can be rewritten using the conversion identity (4.13), the integral representation of the 3-point conformal correlation function (A.7), and the holographic reconstruction formula (4.4):

$$\begin{aligned} & \pi \int_0^{u_3} \frac{du}{u^2} \int_{z_3-i(u-u_3)}^{z_3+i(u-u_3)} dz G_{h_1}(\mathbf{x}, \mathbf{x}_1) G_{h_2}(\mathbf{x}, \mathbf{x}_2) \tilde{G}_{h_3}(\mathbf{x}, \mathbf{x}_3) \\ &= \sum_{n=0}^{\infty} \frac{a(h_3; h_1, h_2; n)}{\gamma_{h_1 h_2 h_{12|n}}} \mathcal{V}_{h_1 h_2 h_{12|n}}(\mathbf{x}_1, \mathbf{x}_2, \mathbf{x}_3), \end{aligned} \quad (\text{B.44})$$

which proves Corollary 1.

#### B.4 Lemma 4

Let us consider the following integral:

$$\lim_{\varepsilon \rightarrow 0} \int_{z_i-iu_i}^{z_i+iu_i} dw_i \int_0^\infty \frac{du}{u^2} \int_{C(\varepsilon)+C_i(\varepsilon)} dz \hat{G}_{h_i}(\mathbf{x}, \mathbf{x}_i, w_i) f(\mathbf{x}), \quad (\text{B.45})$$

where the contour  $C_i(\varepsilon)$  is shown in fig. 6, the sum  $C(\varepsilon) + C_i(\varepsilon)$  is a continuous curve, and  $C(\varepsilon)$  is any contour on the complex  $z$ -plane that avoids possible poles of  $f(\mathbf{x})$  while satisfying  $\text{Re}(z) \neq z_i, \forall z \in C(\varepsilon)$ .

The proof is straightforward: one splits the integral over  $z$  in (B.45) into two integrals over contours  $C(\varepsilon)$  and  $C_i(\varepsilon)$ , then applies Lemma 1 to the integral over  $C(\varepsilon)$  and Lemma 2 to the integral over  $C_i(\varepsilon)$ :

$$\begin{aligned} \lim_{\varepsilon \rightarrow 0} \int_0^\infty \frac{du}{u^2} \int_{C(\varepsilon)} dz G_{h_i}(\mathbf{x}, \mathbf{x}_i) f(\mathbf{x}) &= \pi \int_0^{u_i} \frac{du}{u^2} \int_{z_i-i(u-u_i)}^{z_i+i(u-u_i)} dz \tilde{G}_{h_i}(\mathbf{x}, \mathbf{x}_i) f(\mathbf{x}) \\ &+ \lim_{\varepsilon \rightarrow 0} \int_{z_i-iu_i}^{z_i+iu_i} dw_i \int_0^\infty \frac{du}{u^2} \int_{C(\varepsilon)+C_i(\varepsilon)} dz \hat{G}_{h_i}(\mathbf{x}, \mathbf{x}_i, w_i) f(\mathbf{x}), \end{aligned} \quad (\text{B.46})$$

where  $f(\mathbf{x})$  is subject to the same restriction as in Lemma 2. This proves Lemma 4.

Note that a similar relation between the bulk-to-bulk and modified propagators in Lorentzian  $\text{AdS}_2$  was explicitly found in the  $h_i = 1$  case in [31] (the authors also discussed a generalization to any  $h_i$ )

$$G_h(\mathbf{x}, \mathbf{x}') = \pi \theta(u' - u) \theta(u' - u - |z' - z|) \tilde{G}_h(\mathbf{x}, \mathbf{x}') + i \int_{z'-u'}^{z'+u'} dw \hat{G}_h(\mathbf{x}, \mathbf{x}', w), \quad (\text{B.47})$$

where  $\theta(x)$  is the Heaviside step function. This relation is similar to the conversion identity (4.13) in a domain where the Heaviside step functions vanish

$$G_h(\mathbf{x}, \mathbf{x}') = i \int_{z'-u'}^{z'+u'} dw \widehat{G}_h(\mathbf{x}, \mathbf{x}', w), \quad u > u' - |z' - z|, \quad (\text{B.48})$$

cf. (4.13). By changing  $z' \rightarrow iz'$ ,  $z \rightarrow iz$ ,  $w \rightarrow iw$  and requiring  $z, z' \in \mathbb{R}$  in (4.13) one obtains (B.48).

On the other hand, the superposition identity (4.26) can be obtained from (B.47), although with some limitations. To this end, we integrate the identity (B.47) with a test function over  $\mathbf{x} \in \mathbb{R}_+ \times \mathbb{R}$ , introduce the  $\varepsilon$ -prescription in the bulk-to-bulk propagator to avoid crossing its branch cuts and then make the Wick rotation  $z' \rightarrow iz'$ :

$$\begin{aligned} \int_0^\infty \frac{du}{u^2} \int_{-i\infty}^{i\infty} dz G_h(\mathbf{x}, \mathbf{x}') f(\mathbf{x}) &= \pi \int_0^{u'} \frac{du}{u^2} \int_{z'+i(u'-u)}^{z'-i(u'-u)} dz \widetilde{G}_h(\mathbf{x}, \mathbf{x}') f(\mathbf{x}) \\ &\quad + \int_0^\infty \frac{du}{u^2} \int_{-i\infty}^{i\infty} dz \int_{z'-iu'}^{z'+iu'} dw \widehat{G}_h(\mathbf{x}, \mathbf{x}', w) f(\mathbf{x}), \end{aligned} \quad (\text{B.49})$$

where we also changed the integration variables  $z \rightarrow iz$  and  $w \rightarrow iw$ . The only difference between this identity and the superposition identity (4.26) is the integration contour over  $z$ . By rotating it around the point  $z = 0$  by  $\frac{\pi}{2}$  one transforms this contour into the line contour  $\mathbb{R}$ , which corresponds to choosing  $C(\varepsilon) = \mathbb{R} \setminus U_\varepsilon(z')$  in the superposition identity (4.26). Note that this rotation implies that a test function  $f(\mathbf{x})$  is holomorphic in  $z \in \mathbb{C}$ , whereas the superposition identity allows  $f(\mathbf{x})$  to have singularities outside the integration domain.

## B.5 Lemma 5

Let us consider the following integral

$$\int_0^\infty \frac{du}{u^2} \int_{\mathbb{R}} dz \prod_{i=1}^n G_{h_i}(\mathbf{x}, \mathbf{x}_i) f(\mathbf{x}) = \int_0^\infty \frac{du}{u^2} \int_{\mathbb{R}} dz G_{h_1}(\mathbf{x}, \mathbf{x}_1) g_1(\mathbf{x}), \quad (\text{B.50})$$

where  $f(\mathbf{x})$  on the left-hand side is a test function and the product of  $n - 1$  bulk-to-bulk propagators and the test function  $f(\mathbf{x})$  on the right-hand side is denoted as  $g_1(\mathbf{x})$ . Now, we apply the superposition identity (4.26) to the bulk-to-bulk propagator  $G_{h_1}(\mathbf{x}, \mathbf{x}_1)$  with the contour  $C(\varepsilon_1)$  taken as  $\mathbb{R} \setminus U_{\varepsilon_1}(z_1)$ :

$$\begin{aligned} \lim_{\varepsilon_1 \rightarrow 0} \int_0^\infty \frac{du}{u^2} \int_{\mathbb{R} \setminus U_{\varepsilon_1}(z_1)} dz G_{h_1}(\mathbf{x}, \mathbf{x}_1) g_1(\mathbf{x}) &= \pi \int_0^{u_1} \frac{du}{u^2} \int_{z_1-i(u-u_1)}^{z_1+i(u-u_1)} dz \widetilde{G}_{h_1}(\mathbf{x}, \mathbf{x}_1) g_1(\mathbf{x}) \\ &\quad + \lim_{\varepsilon_1 \rightarrow 0} \int_{z_1-iu_1}^{z_1+iu_1} dw_1 \int_0^\infty \frac{du}{u^2} \int_{\mathbb{R} \setminus U_{\varepsilon_1}(z_1) + C_1(\varepsilon_1)} dz \widehat{G}_{h_1}(\mathbf{x}, \mathbf{x}_1, w_1) g_1(\mathbf{x}). \end{aligned} \quad (\text{B.51})$$

Since  $g_1(\mathbf{x})$  contains the product of bulk-to-bulk propagators, one can again apply the superposition identity to one of the propagators inside  $g_1(\mathbf{x})$ . Rewriting the second term in (B.51), one obtains

$$\begin{aligned} & \lim_{\varepsilon_1 \rightarrow 0} \int_{z_1 - iu_1}^{z_1 + iu_1} dw_1 \int_0^\infty \frac{du}{u^2} \int_{\mathbb{R} \setminus U_{\varepsilon_1}(z_1) + C_1(\varepsilon_1)} dz \widehat{G}_{h_1}(\mathbf{x}, \mathbf{x}_1, w_1) g_1(\mathbf{x}) \\ &= \lim_{\varepsilon_1 \rightarrow 0} \int_{z_1 - iu_1}^{z_1 + iu_1} dw_1 \int_0^\infty \frac{du}{u^2} \int_{\mathbb{R} \setminus U_{\varepsilon_1}(z_1) + C_1(\varepsilon_1)} dz G_{h_2}(\mathbf{x}, \mathbf{x}_2) g_2(\mathbf{x}, w_1), \end{aligned} \quad (\text{B.52})$$

where we denoted the product of  $n - 2$  bulk-to-bulk propagators and the modified propagator  $\widehat{G}_{h_1}$  as  $g_2(\mathbf{x}, w_1)$ .

To apply the superposition identity to the bulk-to-bulk propagator  $G_{h_2}(\mathbf{x}, \mathbf{x}_2)$  one chooses the contour  $C(\varepsilon_2)$  as  $(\mathbb{R} \setminus U_{\varepsilon_1}(z_1) + C_1(\varepsilon_1)) \setminus U_{\varepsilon_2}(z_2)$ . Since  $z_1 \neq z_2$ ,  $\exists \varepsilon$  such that for  $\forall \varepsilon_1 < \varepsilon$  and  $\forall \varepsilon_2 < \varepsilon$ :  $U_{\varepsilon_2}(z_2) \cap C_1(\varepsilon_1) = \emptyset$ . As  $\varepsilon_{1,2} \rightarrow 0$ , we assume that  $\varepsilon_{1,2} < \varepsilon$ , and, therefore, the contour  $C(\varepsilon_2)$  is given by the contour  $C(\varepsilon_1, \varepsilon_2) \equiv \mathbb{R} \setminus (U_{\varepsilon_1}(z_1) \cup U_{\varepsilon_2}(z_2)) + C_1(\varepsilon_1)$ . The result of applying the superposition identity to (B.52) is given by

$$\begin{aligned} & \lim_{\varepsilon_2 \rightarrow 0} \int_0^\infty \frac{du}{u^2} \int_{C(\varepsilon_1, \varepsilon_2)} dz G_{h_2}(\mathbf{x}, \mathbf{x}_2) g_2(\mathbf{x}, w_1) = \pi \int_0^{u_2} \frac{du}{u^2} \int_{z_2 - i(u-u_2)}^{z_2 + i(u-u_2)} dz \widetilde{G}_{h_2}(\mathbf{x}, \mathbf{x}_2) g_2(\mathbf{x}, w_1) \\ &+ \lim_{\varepsilon_2 \rightarrow 0} \int_{z_2 - iu_2}^{z_2 + iu_2} dw_2 \int_0^\infty \frac{du}{u^2} \int_{C(\varepsilon_1, \varepsilon_2) + C_2(\varepsilon_2)} dz \widehat{G}_{h_2}(\mathbf{x}, \mathbf{x}_2, w_2) g_2(\mathbf{x}, w_1). \end{aligned} \quad (\text{B.53})$$

Repeating this procedure  $n - 2$  times and then applying the conversion identity (4.13) to the bulk-to-bulk propagators in the terms with  $\widetilde{G}$  one obtains the multipoint superposition identity (4.27).

## References

- [1] J. M. Maldacena, *The Large  $N$  limit of superconformal field theories and supergravity*, *Adv. Theor. Math. Phys.* **2** (1998) 231–252, [[hep-th/9711200](#)].
- [2] S. Gubser, I. R. Klebanov, and A. M. Polyakov, *Gauge theory correlators from noncritical string theory*, *Phys. Lett.* **B428** (1998) 105–114, [[hep-th/9802109](#)].
- [3] E. Witten, *Anti-de Sitter space and holography*, *Adv. Theor. Math. Phys.* **2** (1998) 253–291, [[hep-th/9802150](#)].
- [4] M. Ammon, A. Castro, and N. Iqbal, *Wilson Lines and Entanglement Entropy in Higher Spin Gravity*, *JHEP* **10** (2013) 110, [[arXiv:1306.4338](#)].
- [5] J. de Boer and J. I. Jottar, *Entanglement Entropy and Higher Spin Holography in  $AdS_3$* , *JHEP* **04** (2014) 089, [[arXiv:1306.4347](#)].
- [6] J. de Boer, A. Castro, E. Hijano, J. I. Jottar, and P. Kraus, *Higher spin entanglement and  $\mathcal{W}_N$  conformal blocks*, *JHEP* **07** (2015) 168, [[arXiv:1412.7520](#)].
- [7] A. Hegde, P. Kraus, and E. Perlmutter, *General Results for Higher Spin Wilson Lines and Entanglement in Vasiliev Theory*, *JHEP* **01** (2016) 176, [[arXiv:1511.05555](#)].

- [8] A. Bhatta, P. Raman, and N. V. Suryanarayana, *Holographic Conformal Partial Waves as Gravitational Open Wilson Networks*, *JHEP* **06** (2016) 119, [[arXiv:1602.02962](https://arxiv.org/abs/1602.02962)].
- [9] M. Besken, A. Hegde, E. Hijano, and P. Kraus, *Holographic conformal blocks from interacting Wilson lines*, *JHEP* **08** (2016) 099, [[arXiv:1603.07317](https://arxiv.org/abs/1603.07317)].
- [10] M. Besken, A. Hegde, and P. Kraus, *Anomalous dimensions from quantum Wilson lines*, [arXiv:1702.06640](https://arxiv.org/abs/1702.06640).
- [11] Y. Hikida and T. Uetoko, *Correlators in higher-spin  $AdS_3$  holography from Wilson lines with loop corrections*, *PTEP* **2017** (2017), no. 11 113B03, [[arXiv:1708.08657](https://arxiv.org/abs/1708.08657)].
- [12] N. Anand, H. Chen, A. L. Fitzpatrick, J. Kaplan, and D. Li, *An Exact Operator That Knows Its Location*, *JHEP* **02** (2018) 012, [[arXiv:1708.04246](https://arxiv.org/abs/1708.04246)].
- [13] Y. Hikida and T. Uetoko, *Superconformal blocks from Wilson lines with loop corrections*, *JHEP* **08** (2018) 101, [[arXiv:1806.05836](https://arxiv.org/abs/1806.05836)].
- [14] Y. Hikida and T. Uetoko, *Conformal blocks from Wilson lines with loop corrections*, *Phys. Rev. D* **97** (2018), no. 8 086014, [[arXiv:1801.08549](https://arxiv.org/abs/1801.08549)].
- [15] M. Besken, E. D'Hoker, A. Hegde, and P. Kraus, *Renormalization of gravitational Wilson lines*, *JHEP* **06** (2019) 020, [[arXiv:1810.00766](https://arxiv.org/abs/1810.00766)].
- [16] A. Bhatta, P. Raman, and N. V. Suryanarayana, *Scalar Blocks as Gravitational Wilson Networks*, *JHEP* **12** (2018) 125, [[arXiv:1806.05475](https://arxiv.org/abs/1806.05475)].
- [17] E. D'Hoker and P. Kraus, *Gravitational Wilson lines in  $AdS_3$* , [arXiv:1912.02750](https://arxiv.org/abs/1912.02750).
- [18] A. Castro, N. Iqbal, and E. Llabrés, *Wilson lines and Ishibashi states in  $AdS_3/CFT_2$* , *JHEP* **09** (2018) 066, [[arXiv:1805.05398](https://arxiv.org/abs/1805.05398)].
- [19] P. Kraus, A. Sivaramakrishnan, and R. Snively, *Late time Wilson lines*, *JHEP* **04** (2019) 026, [[arXiv:1810.01439](https://arxiv.org/abs/1810.01439)].
- [20] A. Blommaert, T. G. Mertens, and H. Verschelde, *The Schwarzian Theory - A Wilson Line Perspective*, *JHEP* **12** (2018) 022, [[arXiv:1806.07765](https://arxiv.org/abs/1806.07765)].
- [21] L.-Y. Hung, W. Li, and C. M. Melby-Thompson, *Wilson line networks in  $p$ -adic  $AdS/CFT$* , *JHEP* **05** (2019) 118, [[arXiv:1812.06059](https://arxiv.org/abs/1812.06059)].
- [22] A. Castro, P. Sabella-Garnier, and C. Zukowski, *Gravitational Wilson Lines in 3D de Sitter*, *JHEP* **07** (2020) 202, [[arXiv:2001.09998](https://arxiv.org/abs/2001.09998)].
- [23] K. Alkalaev and V. Belavin, *More on Wilson toroidal networks and torus blocks*, *JHEP* **11** (2020) 121, [[arXiv:2007.10494](https://arxiv.org/abs/2007.10494)].
- [24] V. Belavin and J. R. Cabezas, *Wilson lines construction of  $osp(1|2)$  conformal blocks*, *Nucl. Phys. B* **985** (2022) 115981, [[arXiv:2204.12149](https://arxiv.org/abs/2204.12149)].
- [25] V. Belavin, P. Oreglia, and J. R. Cabezas, *Wilson lines construction of  $sl3$  toroidal conformal blocks*, *Nucl. Phys. B* **990** (2023) 116186, [[arXiv:2301.04575](https://arxiv.org/abs/2301.04575)].
- [26] A. Castro, I. Coman, J. R. Fliss, and C. Zukowski, *Coupling Fields to 3D Quantum Gravity via Chern-Simons Theory*, *Phys. Rev. Lett.* **131** (2023), no. 17 171602, [[arXiv:2304.02668](https://arxiv.org/abs/2304.02668)].
- [27] K. Alkalaev, A. Kanoda, and V. Khiteev, *Wilson networks in  $AdS$  and global conformal blocks*, *Nucl. Phys. B* **998** (2024) 116413, [[arXiv:2307.08395](https://arxiv.org/abs/2307.08395)].

[28] G. W. Moore and N. Seiberg, *Classical and Quantum Conformal Field Theory*, *Commun. Math. Phys.* **123** (1989) 177.

[29] K. Alkalaev and V. Khiteev, *Holographic reconstruction for AdS Wilson line networks and scalar Witten diagrams*, *JHEP* **07** (2025) 265, [[arXiv:2412.03290](#)].

[30] A. Hamilton, D. N. Kabat, G. Lifschytz, and D. A. Lowe, *Local bulk operators in AdS/CFT: A Boundary view of horizons and locality*, *Phys. Rev. D* **73** (2006) 086003, [[hep-th/0506118](#)].

[31] D. Kabat, G. Lifschytz, and D. A. Lowe, *Constructing local bulk observables in interacting AdS/CFT*, *Phys. Rev. D* **83** (2011) 106009, [[arXiv:1102.2910](#)].

[32] D. Kabat and G. Lifschytz, *Bulk equations of motion from CFT correlators*, *JHEP* **09** (2015) 059, [[arXiv:1505.03755](#)].

[33] D. Kabat and G. Lifschytz, *Dressing bulk fields in  $AdS_3$* , *JHEP* **10** (2020) 189, [[arXiv:2008.01198](#)].

[34] D. Kabat and G. Lifschytz, *Locality, bulk equations of motion and the conformal bootstrap*, *JHEP* **10** (2016) 091, [[arXiv:1603.06800](#)].

[35] T. Banks, M. R. Douglas, G. T. Horowitz, and E. J. Martinec, *AdS dynamics from conformal field theory*, [hep-th/9808016](#).

[36] E. Hijano, P. Kraus, E. Perlmutter, and R. Snively, *Witten Diagrams Revisited: The AdS Geometry of Conformal Blocks*, *JHEP* **01** (2016) 146, [[arXiv:1508.00501](#)].

[37] E. D'Hoker and D. Z. Freedman, *General scalar exchange in  $AdS(d+1)$* , *Nucl. Phys. B* **550** (1999) 261–288, [[hep-th/9811257](#)].

[38] E. D'Hoker, D. Z. Freedman, and L. Rastelli,  *$AdS / CFT$  four point functions: How to succeed at  $z$  integrals without really trying*, *Nucl. Phys. B* **562** (1999) 395–411, [[hep-th/9905049](#)].

[39] H. Liu, *Scattering in anti-de Sitter space and operator product expansion*, *Phys. Rev. D* **60** (1999) 106005, [[hep-th/9811152](#)].

[40] L. Hoffmann, A. C. Petkou, and W. Ruhl, *Aspects of the conformal operator product expansion in  $AdS / CFT$  correspondence*, *Adv. Theor. Math. Phys.* **4** (2002) 571–615, [[hep-th/0002154](#)].

[41] F. A. Dolan and H. Osborn, *Superconformal symmetry, correlation functions and the operator product expansion*, *Nucl. Phys. B* **629** (2002) 3–73, [[hep-th/0112251](#)].

[42] C. Fronsdal, *Elementary particles in a curved space. II*, *Phys. Rev. D* **10** (1974) 589–598.

[43] E. Hijano, P. Kraus, E. Perlmutter, and R. Snively, *Semiclassical Virasoro blocks from  $AdS_3$  gravity*, *JHEP* **12** (2015) 077, [[arXiv:1508.04987](#)].

[44] E. Hijano, P. Kraus, and R. Snively, *Worldline approach to semi-classical conformal blocks*, *JHEP* **07** (2015) 131, [[arXiv:1501.02260](#)].

[45] M. Nishida and K. Tamaoka, *Geodesic Witten diagrams with an external spinning field*, *PTEP* **2017** (2017), no. 5 053B06, [[arXiv:1609.04563](#)].

[46] H.-Y. Chen, E.-J. Kuo, and H. Kyono, *Anatomy of Geodesic Witten Diagrams*, *JHEP* **05** (2017) 070, [[arXiv:1702.08818](#)].

[47] A. Castro, E. Llabrés, and F. Rejon-Barrera, *Geodesic Diagrams, Gravitational Interactions & OPE Structures*, *JHEP* **06** (2017) 099, [[arXiv:1702.06128](#)].

[48] E. Dyer, D. Z. Freedman, and J. Sully, *Spinning Geodesic Witten Diagrams*, *JHEP* **11** (2017) 060, [[arXiv:1702.06139](#)].

[49] C. Sleight and M. Taronna, *Spinning Witten Diagrams*, *JHEP* **06** (2017) 100, [[arXiv:1702.08619](#)].

[50] K. Tamaoka, *Geodesic Witten diagrams with antisymmetric tensor exchange*, *Phys. Rev. D* **96** (2017), no. 8 086007, [[arXiv:1707.07934](#)].

[51] M. Nishida and K. Tamaoka, *Fermions in Geodesic Witten Diagrams*, *JHEP* **07** (2018) 149, [[arXiv:1805.00217](#)].

[52] S. Parikh, *Holographic dual of the five-point conformal block*, *JHEP* **05** (2019) 051, [[arXiv:1901.01267](#)].

[53] C. B. Jepsen and S. Parikh, *Propagator identities, holographic conformal blocks, and higher-point AdS diagrams*, *JHEP* **10** (2019) 268, [[arXiv:1906.08405](#)].

[54] A. L. Fitzpatrick, J. Kaplan, and M. T. Walters, *Universality of Long-Distance AdS Physics from the CFT Bootstrap*, *JHEP* **1408** (2014) 145, [[arXiv:1403.6829](#)].

[55] T. Hartman, *Entanglement Entropy at Large Central Charge*, [arXiv:1303.6955](#).

[56] C. T. Asplund, A. Bernamonti, F. Galli, and T. Hartman, *Holographic Entanglement Entropy from 2d CFT: Heavy States and Local Quenches*, *JHEP* **1502** (2015) 171, [[arXiv:1410.1392](#)].

[57] K. B. Alkalaev and V. A. Belavin, *Classical conformal blocks via AdS/CFT correspondence*, *JHEP* **08** (2015) 049, [[arXiv:1504.05943](#)].

[58] K. B. Alkalaev and V. A. Belavin, *Monodromic vs geodesic computation of Virasoro classical conformal blocks*, *Nucl. Phys. B* **904** (2016) 367–385, [[arXiv:1510.06685](#)].

[59] K. B. Alkalaev, *Many-point classical conformal blocks and geodesic networks on the hyperbolic plane*, *JHEP* **12** (2016) 070, [[arXiv:1610.06717](#)].

[60] P. Banerjee, S. Datta, and R. Sinha, *Higher-point conformal blocks and entanglement entropy in heavy states*, *JHEP* **05** (2016) 127, [[arXiv:1601.06794](#)].

[61] K. B. Alkalaev and V. A. Belavin, *Holographic interpretation of 1-point toroidal block in the semiclassical limit*, *JHEP* **06** (2016) 183, [[arXiv:1603.08440](#)].

[62] K. Alkalaev and M. Pavlov, *Perturbative classical conformal blocks as Steiner trees on the hyperbolic disk*, *JHEP* **02** (2019) 023, [[arXiv:1810.07741](#)].

[63] P. Kraus, A. Maloney, H. Maxfield, G. S. Ng, and J.-q. Wu, *Witten Diagrams for Torus Conformal Blocks*, *JHEP* **09** (2017) 149, [[arXiv:1706.00047](#)].

[64] X. Zhou, *Recursion Relations in Witten Diagrams and Conformal Partial Waves*, *JHEP* **05** (2019) 006, [[arXiv:1812.01006](#)].

[65] S. Giombi, H. Khanchandani, and X. Zhou, *Aspects of CFTs on Real Projective Space*, *J. Phys. A* **54** (2021), no. 2 024003, [[arXiv:2009.03290](#)].

[66] A. Castro and P. J. Martinez, *Revisiting extremal couplings in AdS/CFT*, *JHEP* **12** (2024) 157, [[arXiv:2409.15410](#)].

[67] D. Z. Freedman, S. D. Mathur, A. Matusis, and L. Rastelli, *Correlation functions in the CFT( $d$ ) / AdS( $d+1$ ) correspondence*, *Nucl. Phys. B* **546** (1999) 96–118, [[hep-th/9804058](#)].

- [68] R. Penrose, *Angular momentum; an approach to combinatorial space time*. Quantum Theory and Beyond. Cambridge University Press, Cambridge, 1971.
- [69] M. Ammon, J. Hollweck, T. Hössler, and K. Wölfle, *Thermal n-Point Conformal Blocks in Four Dimensions from Oscillator Representations*, [arXiv:2507.22974](https://arxiv.org/abs/2507.22974).
- [70] H. Bateman and A. Erdélyi, *Higher transcendental functions*. California Institute of technology. Bateman Manuscript project. McGraw-Hill, New York, NY, 1953.
- [71] K. Matsumoto, *Appell and Lauricella Hypergeometric Functions*, p. 79–100. Cambridge University Press, 2020.
- [72] S. I. Bezrodnykh, *Analytic continuation of the Appell function  $F_1$  and integration of the associated system of equations in the logarithmic case*, *Computational Mathematics and Mathematical Physics* **57** (2017) 559–589.